Daytime formation of nitrous acid at a coastal remote site in Cyprus indicating a common ground source of atmospheric HONO and NO

Hannah Meusel, Uwe Kuhn[1], Andreas Reiffs[2], Chinmay Mallik[2], Hartwig Harder[2], Monica Martinez[2], Jan Schuladen[2], Birger Bohn[3], Uwe Parchatka[2], John N. Crowley[2], Horst Fischer[2], Laura Tomsche[2], Anna Novelli[2,3], Thorsten Hoffmann[4], Ruud Janssen[2,], Oscar Hartogensis[5], Michael Pikridas[6], Mihalis Vrekoussis[6,7,8], Efstratios Bourtsoukidis[2], Bettina Weber[1], Jos Lelieveld[2], Jonathan Williams[2], Ulrich Pöschl[1], Yafang Cheng[1], Hang Su[1]

[1]Max Planck institute for Chemistry, Multiphase Chemistry Department, Mainz, Germany
[2]Max Planck Institute for Chemistry, Atmospheric Chemistry Department, Mainz, Germany
[3]Institute for Energy and Climate Research (IEK-8), Research Center Jülich, Jülich, Germany
[4]Johannes Gutenberg University, Inorganic and Analytical Chemistry, Mainz, Germany
[5]Wageningen University and Research Center, Meteorology and Air Quality, Wageningen, Netherlands
[6]Cyprus Institute, Energy, Environment and Water Research Center, Nicosia, Cyprus
[7] Institute of Environmental Physics and Remote Sensing – IUP, University of Bremen, Germany
[8] Center of Marine Environmental Sciences – MARUM, University of Bremen, Germany

Correspondence to: Hang Su (h.su@mpic.de)

Abstract. Characterization of daytime sources of nitrous acid (HONO) is crucial to understand atmospheric oxidation and radical cycling in the planetary boundary layer. HONO and numerous other atmospheric trace constituents were measured on the Mediterranean island of Cyprus during the CYPHEX campaign (CYPHEX = CYprus PHotochemical EXperiment) in summer 2014. Average volume mixing ratios of HONO were 35 pptv (±25 pptv) with a HONO/NO_x ratio of 0.33, which was considerably higher than reported for most other rural and urban regions. Diel profiles of HONO showed peak values in the late morning (60±28 pptv around 09:00 local time), and persistently high mixing ratios during daytime (45±18 pptv) indicating that the photolytic loss of HONO is compensated by a strong daytime source. Budget analyses revealed unidentified sources producing up to 3.4 x 10^6 molecules cm^{-3} s^{-1} of HONO and up to 2.0 x 10^7 molecules cm^{-3} s^{-1} NO. Under humid conditions (RH >70%), the source strengths of HONO and NO exhibited a close linear correlation (R^2=0.72), suggesting a common source that may be attributable to emissions from microbial communities on soil surfaces.

1 Introduction

Nitrous acid (HONO) is an important component of the nitrogen cycle being widely spread in the environment. Either in its protonated form (HONO or HNO_2) or as nitrite ions (NO_2^-) it can be found in the gas phase, on aerosol-particles, in clouds and dew droplets but also in soil, sea-water and sediments (Foster et al., 1990; Rubio et al., 2002; Acker et al., 2005 and 2008; Bianchi et al., 1997). It plays a key role in the oxidizing capacity of the atmosphere, as it is an important precursor of the OH radical, which initiates most atmospheric oxidations. OH radicals react with pollutants in the atmosphere to form mostly less toxic compounds (e.g. CO + OH → CO_2 + H_2O; Levy, 1971). Volatile organic compounds (VOCs) react with OH contributing to formation of secondary aerosols (SOA), which

can serve as cloud condensation nuclei CCN (Arey et al., 1990; Duplissy et al., 2008). Furthermore OH oxidizes SO_2 to H_2SO_4, which condense subsequently to form aerosol particles (Zhou et al. 2013). In this way HONO has an indirect effect on the radiative budget and climate. In the first 2-3 hours following sunrise, when OH production from other sources (photolysis of O_3 and formaldehyde) is relatively low, photolysis of HONO can be the major source of OH radicals as HONO concentrations may be high after accumulation during night time (Lammel and Cape, 1996; Czader et al., 2012; Mao et al., 2010). On average up to 30% of the daily OH budget in the boundary layer is provided by HONO photolysis (Alicke et al., 2002; Kleffmann et al., 2005; Ren et al., 2006), but has been reported as high as 56% (Ren et al., 2003) with ambient HONO mixing ratios ranging from several pptv in rural areas up to a few ppb in highly polluted regions (Acker et al., 2006a and 2006b; Costabile et al., 2010; Li et al., 2012; Michoud et al., 2014; Spataro et al., 2013; Su et al. 2008a; Zhou et al., 2002a).

In early studies, atmospheric HONO was assumed to be in at photostationary state during daytime controlled by the gas phase reaction of NO and OH (R1) and two loss reactions which are the photolysis (R2) and the reaction with OH (R3).

$$OH + NO \rightarrow HONO \quad \text{(R1)}$$

$$HONO \xrightarrow{hv\ (300-405\ nm)} OH + NO \quad \text{(R2)}$$

$$HONO + OH \rightarrow NO_2 + H_2O \quad \text{(R3)}$$

However, field measurements in remote and rural locations, as well as urban and polluted regions found several times higher daytime HONO concentrations than model predictions, suggesting a large unknown source (Kleffmann et al., 2003 and 2005; Su et al., 2008a; Soergel et al., 2011a; Su et al., 2011; Michoud et al., 2014; Czader et al., 2012; Wong et al., 2013; Tang et al., 2015; Oswald et al., 2015) even after considering direct emission of HONO from combustion sources (Kessler and Platt, 1984; Kurtenbach et al., 2001). Heterogeneous reactions on aerosols have been proposed as an explanation for the missing source. The hydrolysis (R4, Finlayson-Pitts et al., 2003) and redox reactions of NO_2 have been intensively investigated on different kinds of surfaces such as fresh soot, aged or organic-coated particles (Ammann et al., 1998; Arens et al., 2001; Aubin et al., 2007; Bröske et al., 2003; Han et al., 2013; Kalberer et al., 1999; Kleffmann et al., 1999; Kleffmann and Wiesen, 2005; Lelievre et al., 2004). Minerals like SiO_2, $CaCO_3$, CaO, Al_2O_3, and Fe_2O_3 showed a catalytic effect on the hydrolysis of NO_2 (Kinugawa et al., 2011; Liu et al., 2015; Wang et al., 2003; Yabushita et al., 2009). Different kind of surfaces (humic acid and other organic compounds, titanium dioxide, soot) can be photochemically activated which leads to enhanced NO_2 uptake and HONO production (R5,George et al., 2005; Langridge et al., 2009; Monge et al., 2010; Ndour et al., 2008; Ramazan et al., 2004; Stemmler et al., 2007; Kebede et al., 2013). The photolysis of particulate nitric acid (HNO_3), nitrate (NO_3^-) and nitro-phenols (R-NO_2) lead to HONO formation as well (Baergen and Donaldson, 2013; Bejan et al., 2006; Ramazan et al., 2004; Scharko et al., 2014; Zhou et al., 2003; Zhou et al., 2011). But these reactions cannot account for the HONO levels observed during daytime (Elshorbany et al., 2012).

$$2\,NO_2 + H_2O \rightarrow HONO + HNO_3 \quad \text{(R4)}$$

$$surface \xrightarrow{hv} e^- \xrightarrow{NO_2} NO_2^- \xrightarrow{H_2O} HONO + OH^- \quad \text{(R5)}$$

On the other hand, soil nitrite, either biogenic or non-biogenic, has been suggested as an effective source of HONO (Su et al., 2011; Oswald et al., 2013; Mamtimin et al., 2016). Depending on soil properties such as pH and water content and according to Henry´s law HONO can be released (Donaldson et al., 2014b; Su et al., 2011). This is consistent with field flux measurements showing HONO emission from the ground rather than deposition as is the case for HNO_3 (Harrison and Kitto, 1994; Kleffmann et al., 2003; Ren et al., 2011; Stutz et al., 2002; VandenBoer et al., 2013; Villena et al., 2011; Zhou et al., 2011). In a recent study, Weber et al. (2015) measured large HONO- and NO-emissions from dryland soils with microbial surface communities (so-called biological soil crusts). Many studies have shown decreasing HONO mixing ratios with altitude in the lowest few hundred meters of the troposphere, due to respective short atmospheric lifetime compared to vertical transport time (Wong et al., 2012 and 2013; Vogel et al., 2003; VandenBoer et al., 2013; Zhang et al., 2009; Young et al., 2012). According to the modelling results of Wong et al. 2013, we estimate that the ground HONO source could be important for up to 200–300 m a.g.l. This indicates that HONO is more relevant for the OH budget close to the surface than in high altitude air masses.

Several field studies also show a correlation of the unknown HONO source with solar radiation or the photolysis frequency of NO_2 J_{NO2} (Su et al., 2008a; Soergel et al., 2011a; Wong et al., 2012; Costabile et al., 2010; Michoud et al., 2014; Oswald et al., 2015; Lee et al., 2016). This correlation can be explained either by the aforementioned photosensitized reactions or by temperature-dependent soil-atmosphere exchange (Su et al., 2011). According to Su et al. (2011), the release of HONO from soil surfaces is controlled by both the soil (biogenic and chemical) production of nitrite and the gas-liquid phase equilibrium. The solubility is strongly temperature-dependent, resulting in a higher HONO emission during noon time and high radiation J_{NO2} periods, and lower HONO emissions or even HONO deposition during the nighttime as further confirmed by VandenBoer et al. (2015). This temperature dependence not only exists for equilibrium over soil solution but also exists for adsorption/desorption equilibrium over dry and humid soil surfaces (Li et al., 2016).

In this study we measured HONO and a suite of other atmospherically relevant trace gases in a coastal area on the Mediterranean Island Cyprus in summer 2014. Due to low local anthropogenic impact and low NOx levels in aged air masses, but high solar radiation, this is an ideal site to investigate possible HONO sources and to gain a better understanding of HONO chemistry.

2 Instrumentation

HONO was measured with a commercial Long Path Absorption Photometry instrument (effective light path 1.5 m, LOPAP, Quma, Wuppertal, Germany). LOPAP has a collecting efficiency of >99% for HONO and a detection limit of 4 pptv at a time resolution of 30s. To avoid potential interferences induced by long inlet lines and heterogeneous formation or loss of HONO on the inlet walls, respectively (Kleffmann et al., 1998; Zhou et al., 2002b; Su et al., 2008b), HONO was collected by a sampling unit installed directly in the outdoor atmosphere, i.e., placed on a mast at a height of 5.8 meters above ground installed at the edge of a laboratory container. Furthermore, the LOPAP has two stripping coils placed in series to reduce known interfering signals (Heland et al., 2001). In the first stripping coil HONO is quantitatively collected. Due to the acidic stripping solution interfering species are collected less efficiently but in both channels. The true concentration of HONO is obtained by subtracting the inferences quantified

in the second channel (in this study average 1 pptv, at most 5 pptv) from the total signal obtained from the first channel. For a more detailed description of LOPAP, see Heland et al. (2001). This correction of chemical interferences ascertained excellent agreement with the (absolute) DOAS measurements, both in a smog chamber and under urban atmospheric conditions (Kleffmann et al., 2006). A possible interference from peroxynitric acid (HNO_4) has been proposed (Liao et al., 2006; Kerbrat et al., 2012; Legrand et al., 2014), but this will be insignificant at the high temperatures during CYPHEX, at which HNO_4 is unstable. The stripping coils are temperature controlled by a water-based thermostat and the whole external sampling unit is shielded from sunlight by a small plastic housing. The reagents were all high purity grade chemicals, i.e., hydrochloric acid (37%, for analysis; Merck), sulfanilamide (for analysis, >99%; AppliChem) and N-(1-naphthyl)-ethylenediamine dihydrochloride (for analysis, >98%; AppliChem). For calibration Titrisol® 1000 mg NO_2^- ($NaNO_2$ in H_2O; Merck) was diluted to 0.0015 and 0.005 mg/L NO_2^-. For preparation all solutions and for cleaning of the absorption tubes 18 MΩ H_2O was used. The accuracy of the HONO measurements was 10%, based on the uncertainties of liquid and gas flow, concentration of calibration standard and regression of calibration.

NO and NO_2 measurements were made with a modified commercial chemiluminescence Detector (CLD 790 SR) originally manufactured by ECO Physics (Duernten, Switzerland). The two-channel CLD based on the chemiluminescence of the reaction between NO and O_3 was used for measurements of NO and NO_2. NO_2 was measured as NO using a photolytic converter from Droplet Measurement Technologies, Boulder USA. In current study, data were obtained at a time resolution of 5 seconds. The CLD detection limits (determined by continuously measuring zero air at measuring site) for NO and NO_2 measurements were 5 pptv and 20 pptv, respectively for an integration period of 5 s. O_3 was measured with a standard UV photometric detector (Model 49, Thermo Environmental Instruments Inc.) with a detection limit of 1 ppb. Data are reported for an integration period of 60 s. The total uncertainties (2σ) for the measurements of NO, NO_2 and O_3 were determined to be 20%, 30% and 5%, respectively, based on the reproducibility of in-field background measurements, calibrations, the uncertainties of the standards and the conversion efficiency of the photolytic converter (Li et al., 2015).

OH and HO_2 radicals were measured using the HydrOxyl Radical measurement Unit based on fluorescence Spectroscopy (HORUS) setup developed at the Max Planck Institute for Chemistry (Mainz, Germany). HORUS is based on laser induced fluorescence- fluorescence assay by gas expansion (LIF-FAGE) technique, wherein OH radicals are selectively excited at low pressure by pulsed UV light at around 308 nm, and the resulting fluorescence of OH is detected using gated microchannel plate (MCP) detectors (Martinez et al., 2010; Hens et al., 2014). The HORUS instrument had an inlet pre-injector (IPI) (Novelli at al. 2014) which allows the periodic addition of propane to scavenge the atmospheric OH radicals. This procedure allows the removal of potential interference species. HO_2 is estimated by converting atmospheric HO_2 into OH using NO, and detecting the additional OH formed. The instrument is calibrated by measuring signals from known amounts of OH and HO_2 generated by photolysis of water vapor in humidified zero air. The accuracy (2 sigma) of the OH measurements was 29% and the precision (1 sigma) was 4.8×10^5 molecules cm^{-3}.

Photolysis frequencies were determined using a spectroradiometer (Metcon GmbH) with a single monochromator and 512 pixel CCD-array as detector (275-640 nm). The thermostatted monochromator/detector unit was attached via a 10 m optical fiber to a 2-Π integrating hemispheric quartz dome. The spectroradiometer was calibrated prior to the

campaign using a 1000 W NIST traceable irradiance standard. J-values were calculated using molecular parameters recommended by the IUPAC and NASA evaluation panels (Sander et al., 2011; IUPAC, 2015). The J-value for HONO was not corrected for upwelling UV radiation and is estimated to have an uncertainty of ~10 % (Bohn et al., 2008).

Aerosol measurements were also performed during the campaign. In this study particulate nitrate and aerosol surface data were used. These were detected by high resolution – time of flight – aerosol mass spectrometer (HR-ToF-AMS, Aerodyne Research Inc., Billerica, MA USA) and scanning mobility particle sizer (SMPS 3936, TSI, Shoreview, MN USA) and aerodynamic particle sizer (APS 3321, TSI), respectively. The mobility and aerodynamic based size distributions were combined based on the algorithm proposed by Khlystov et al. (2004).

The volatile organic compounds (VOC) including α-pinene, β-pinene, isoprene, Δ3-carene, limonene and DMS (dimethyl sulfide) were detected by a commercial Gas Chromatography-Mass Spectrometry (GC-MS) system (MSD 5973; Agilent Technologies GmbH) coupled with an air sampler and a thermal desorber unit (Markes International GmbH). The VOCs were trapped at 30^{o}C on a low-dead-volume quartz cold trap (U-T15ATA; Markes International GmbH) filled with two bed sorbent (Tenax TA and Carbograph I). The cold trap was heated to 320^{o}C and the sample was transferred to a 30m GC column (DB-624, 0.25mm I.D., 1.4μm film; J&W Scientific). The temperature of the GC oven was programmed to be stable at 40^{o}C for 5mins and then rising with a rate of 5^{o}C/min up to 140^{o}C. Following, the rate was increased to 40^{o}C/min up to 230^{o}C where it was stabilized for 3min. Each sample was taken every 45mins and calibrations, using a commercial gas standard mixture (National Physical Laboratory, UK), were performed every 8-12 samples.

Carbon monoxide was measured by infrared absorption spectroscopy using a room temperature quantum cascade laser at a time resolution of 1 s. Data are reported as 60 s averages with a total uncertainty of ~10% mainly determined by the uncertainty of the used NIST standard (Li et al., 2015).

Meteorological parameters (temperature, relative humidity, wind speed and wind direction, pressure, solar radiation, precipitation) were detected by the weather station Vantage Pro2 from DAVIS.

Besides GC-MS all other operating instruments had time resolutions between 20 s and 5 min. For most analyses in this study the data were averaged to 10 min. When GC-MS data were included in the evaluation 1 hour averaged data were used.

3 Site description

Cyprus is a 9251 km² island in the South-East Mediterranean Sea (fig. 1). The measuring site was located on a military compound in Ineia, Cyprus (N 34.9638, E 32.3778), about 600 m above sea level and approximately 5.5 - 8 km from the coast line (in the main wind direction W-SW). The field site is characterized by light vegetation cover, mainly comprising small shrubs like *Pistacia lentiscus*, *Sacopoterium spinosum*, and *Nerium oleander*, herbs like *Inula viscosa* and *Foeniculum vulgare* and few typical Mediterranean trees like *Olea europaea*, *Pinus* sp., *and Ceratonia siliqua*.. The area within a radius of about 15 km around the station is only weakly populated. Paphos (88,266 citizens) is located 20 km south of the field site, Limassol (235,000), Nicosia (325,756) and Larnaca (143,367) are 70, 90 and 110 km in the E-SE, respectively (population data according to statistical service of the

republic of Cyprus, www.cystat.gov.cy, census of population Oct 2011). During the campaign (07.07. - 04.08.2014), clear sky conditions prevailed and occasionally clouds skimmed the site. No rain was observed, but the elevated field site was impacted by fog during nighttime and early morning due to adiabatic cooling of ascending marine humid air masses. Temperature ranged from 18 to 28°C. Within the main local wind direction of SW (fig. 2A) there was no direct anthropogenic influence resulting in clean humid air from the sea. Analysis of 48-hours back trajectories showed mainly two source regions of air mass origin (fig. 2B). Approximately half (46%) of the campaign the air masses came from the West of Cyprus spending most of their time over the Mediterranean Sea prior to arriving at the site. During the remaining half of the campaign air masses originated from the North of Cyprus, from East European countries (Turkey, Bulgaria, Rumania, Ukraine and Russia). Westerly air masses have been shown to exhibit lower concentration of gaseous and aerosol pollutants than the predominant northerly air masses that typically reach the site (Kleanthous et al., 2014). They spent more time over continental terrestrial surface and were likely to be additionally affected by biomass burning events detected in East Europe within the measurement periods (FIRMS, MODIS, web fire mapper, fig. S1). Previous back trajectory studies in the eastern Mediterranean support this assumption (Kleanthous et al., 2014; Pikridas et al., 2010).

Most of the time the advected air mass was loaded with high humidity as a result of sea breeze circulation. Two periods of about 4 days with lower relative humidity occurred. These two situations will be contrasted below.

4 Results

The concentrations of HONO and other atmospheric trace gases as well as meteorological conditions observed on Cyprus from 7th July 2014 to 3rd August 2014 are shown in fig. 3. In general, low trace gas mixing ratios were indicative of clean marine atmospheric boundary conditions, as pollutants are oxidized by OH during the relatively long air transport time over the Mediterranean sea (more than 30 h), and without significant impact of direct anthropogenic emissions.

Ambient HONO mixing ratios ranged from below detection limit (< 4 pptv) to above 300 pptv. Daily average HONO was 35 pptv (± 25 pptv; 1σ standard deviation, following alike). The daily average NO_2 and NO mixing ratios were 140 ± 115 and 20 ± 35 pptv respectively, but showed intermittent peaks up to 50 ppbv when sampling air was streamed from the diesel generator used to power the station, from the access route or the parking lot by local winds (easterly, fig S2). These incidents, which account for 4% of the campaign time, were classified as local air pollution events and were omitted from analysis. Mean O_3 and CO mixing ratios were 72 ± 12 ppb and 98 ± 11 ppbv respectively. OH radicals ranged from below detection limit ($1x10^5$ molecules cm^{-3}) during nighttime to $8x10^6$ molecules cm^{-3} during daytime (see fig. S3). Daytime HO_2/OH ratio ranged from 100 to 150. The mixing ratios of NO_2, O_3 and CO varied in unison, and were significantly ($p<0.05$) higher during periods when air masses originated from East Europe (brownish bar in fig. 3a lower panel), indicative of air pollution and shorter transport times compared to western Europe (NO_2: Northerly: 144 ± 130 pptv, westerly: 127 ± 106 pptv; O_3: Northerly: 74 ± 11 ppbv, westerly: 66 ± 12 ppbv; CO: Northerly: 101 ± 9 ppbv, westerly: 90 ± 10 ppbv). In contrast, NO and HONO mixing ratios were slightly higher when air masses came from Western Europe and over the sea (NO: Northerly: 17 ± 35 pptv, westerly: 20 ± 44 pptv; HONO: Northerly: 32 ± 26 pptv, westerly: 38 ± 22 pptv).

Besides two different air mass origins, two periods with different behaviour of relative humidity were identified illustrated by blue and yellow boxes in fig. 3(a and b). In both periods we found northerly and westerly air mass origins. The diel profiles of trace gas mixing ratios and meteorological variables of the humid period (blue box) are shown in Fig. 4a, the ones of the dry period (yellow box) in Fig 4b. During the drier period HONO concentrations are stable and low (6 pptv) during night, while mean nighttime HONO mixing ratios during the humid period (fig. 4a) showed an expected slow increase of about 20 pptv (from 20 to 40 pptv), as anticipated from heterogeneous production and accumulation within a nocturnal boundary layer characterized by a stable stratification and low wind speed (Acker et al., 2005; Su et al., 2008b; Li et al., 2012). During both periods, but more pronounced in the drier period, HONO rapidly increased by a factor of 2 within two hours after sunrise and then slowly decreased until sunset. Similar profiles were also observed for other trace gases like isoprene or DMS which are transported in upslope winds. Strong HONO morning peaks and high daytime mixing ratios suggest a strong daytime source, compensating the short atmospheric lifetime (15 min) caused by fast photolysis.

Mean NO mixing ratios were close to the detection limit (5 pptv) during night and increased after sunrise (06:00 local time LT) to mean values of 60 pptv (peak 150 pptv) at 09:00 LT, prior to declining for the rest of the day until sunset (20:00 LT). In the absence of local NO sources low nighttime values are a result of the conversion of NO to NO_2 by O_3 which was continuously high (Beygi et al., 2011). The diel profiles of NO mixing ratios followed closely those of HONO mixing ratios. This similarity and their dependency on relative humidity are suggestive of a common source for both reactive nitrogen species.

NO_2 mixing ratios were somewhat lower during nighttime, but in general the diel variability remained in a narrow range between 100 and 200 pptv. Likewise, the diel courses of O_3 and CO mixing ratios revealed relatively low day/night variability in a range of 65-75 and 90-100 ppb, respectively.

5 Discussion

Low NO_x conditions at this remote field site in photochemically aged marine air were found to be an ideal prerequisite to trace yet un-defined local HONO sources. On Cyprus, diel profiles of HONO showed peak values in the late morning and persistently high mixing ratios during daytime, as has been reported for some other remote regions (Acker et al., 2006a; Zhou et al., 2007; Huang et al., 2002). This is not the case for rural and urban sites, where atmospheric HONO mixing ratios are normally observed to continuously build up during nighttime presumably due to heterogeneous reactions involving NO_x and decline in the morning due to strong photodissociation (e.g., Elshorbany et al., 2012 and references therein).

The diel HONO/NO_x ratio (fig. 4a+b, third panel) shows consistently high values during the humid period (fig. 4a) and significant diel variation for the dry case (fig. 4b) with higher values during day. The ratio (average 0.33 and peak values greater than 2) is higher than that reported for most other regions, suggesting a strong impact of local HONO sources. Elshorbany et al. (2012) investigated data from 15 different urban and rural field measurement campaigns around the globe, and came up with a robust representative mean atmospheric HONO/NOx ratio as low as 0.02. However, high values were observed at remote mountain sites, with mean values of 0.23 (up to ≈0.5 in the late morning; Zhou et al., 2007) or 0.2–0.4 at remote arctic/polar sites (Li, 1994; Zhou et al., 2001; Beine et al.,

2001; Jacobi et al., 2004; Amoroso et al., 2010). Legrand et al. (2014) observed HONO/NO_x ratios between 0.27 and 0.93 during experiments with irradiated Antarctic snow depending on radiation wavelength, temperature and nitrate content. Elevated HONO/NO_x ratios at low NO_x levels show the importance of HONO formation mechanisms other than heterogeneous NO_x reactions.

5.1 Nighttime HONO accumulation

Between 18:30 – 7:30 LT HONO has an atmospheric lifetime of more than 45 min and [OH] is low, just about $1x10^5$ molecules cm^{-3}, so that the calculation of HONO at photostationary state $[HONO]_{pss}$ (R1-R3) at night is not appropriate. Instead, nighttime HONO concentrations can be estimated due to heterogeneous reaction of NO_2 described in Eq. (1) (Alicke et al., 2002+2003; Su et al., 2008b; Soergel et al., 2011b). Three studies in different environments from a rural forest region in East Germany (Soergel et al., 2011b) and a non-urban site in the Pearl River delta, China (Su et al., 2008b) to an urban, polluted site in Beijing (Spataro et al., 2013) found a conversion rate of about 1.6% h^{-1} (1.1-1.8 % h^{-1}).

$$[HONO]_{het} = [HONO]_{evening} + 0.016\ h^{-1}[NO_2]\ \Delta t, \qquad \text{(Eq. 1)}$$

$[HONO]_{het}$ denotes the accumulation of HONO by heterogeneous conversion of NO_2, $[HONO]_{evening}$ the measured HONO concentration at 20:30 LT, $[NO_2]$ the measured average NO_2 concentration between 20:30 and 7:30 LT, Δt time span in hours.

Measured and calculated HONO mixing ratios are compared in figure 4 (upper panel). During the humid period, during night the estimated (according Eq. (1), fig. 4a upper panel, grey line) and observed HONO mixing ratios are in good agreement ($R^2 = 0.9$). During the drier period the observed HONO mixing ratios were lower than the ones calculated with a NO_2 conversion rate of 1.6% h^{-1}. Here the approach for the nighttime conversion frequency by e.g. Alicke et al., 2002+2003, Su et al., 2008b or Soergel et al., 2011b ($\text{rate} = \frac{HONO_{t2} - HONO_{t1}}{\Delta t * \overline{NO_2}}$) was used. The 7 days average conversion rate for the dry nights was 0.36% h^{-1} (fig. 4b, upper panel, black line), comparable to results of Kleffmann et al. (2003) reporting a conversion rate of $6x10^{-7}$ s^{-1} (0.22% h^{-1}) for rural forested land in Germany.

As already mentioned above, it is apparent that under low RH conditions during night, HONO mixing ratios were much lower than under humid conditions, and HONO morning peaks were most pronounced (compare Fig. 4a and 4b: humid/dry). Both HONO (Donaldson et al., 2014a) and NO_2 (Wang et al., 2012; Liu et al., 2015) uptake coefficients have recently been reported to be much stronger for dry soil, or at low RH, respectively, which is in line with HONO on Cyprus being close to the detection limit in nights with low relative humidity. On the other hand, it has been shown on glass and on soil proxies that the yield of HONO formation from NO_2 on surfaces is low under dry conditions, but sharply increases at RH >30% (Liu et al., 2015) or >60% (Finlayson-Pitts et al., 2003). On Cyprus the strong morning HONO peaks after dry nights were accompanied by an increase in relative humidity from 40 to 80%. Deposited and accumulated NO_2 on dry soil surfaces could be released as HONO at high rates under elevated RH conditions. In contrast, in a humid regime HONO mixing ratios were continuously high during nighttime and showed less pronounced morning peaks, suggesting lower nighttime deposition of NO_2 and lower HONO emissions in the morning, respectively.

As morning HONO peak mixing ratios were most pronounced after dry nights on Cyprus, our observations are to some extent contradictory to earlier results that have proposed that dew formation on the ground surface may be responsible for HONO nighttime accumulation in the aqueous phase, followed by release from this reservoir after dew evaporation the next morning (Zhou et al., 2002a, Rubio et al., 2002, He et al., 2006). We cannot rule out that the latter could have contributed to nighttime accumulation of HONO during humid conditions, as we had no means to measure dew formation at the site, and high daytime HONO mixing ratios were observed under all humidity regimes. However, kinetic models of competitive adsorption of trace gases and water onto particle surfaces predict exchange behavior explicitly distinct from the liquid phase (Donaldson et al., 2014a). The nitrogen composition in thin water films (few water molecular monolayers) is complex, including HONO, NO, HNO_3, water–nitric acid complexes, NO_2^+ and N_2O_4 (Finlayson-Pitts et al., 2003). With only small amounts of surface-bound water, nitric acid is largely undissociated HNO_3 and is assumed to be stabilized upon formation of the HNO_3–H_2O complexes (hydrates), which have unique reactivity compared to nitric acid water aqueous solutions, where it is dissociated H^+ and NO_3^- ions (Finlayson-Pitts et al., 2003). Likewise, HONO formation rates in surface bound water are about four orders of magnitude larger than expected for the aqueous phase reaction (Pitts et al., 1984).

Diel HONO profiles very similar to those on Cyprus with a late morning maximum and late afternoon/early evening minimum have been observed at the Meteorological Observatory Hohenpeissenberg, a mountain-top site in Germany (Acker et al., 2006a) and by Zhou et al. (2007) at the summit of Whiteface Mountain in New York State. For the latter study, formation of dew could be ruled out as relative humidity was mostly well below saturation. Zhou et al. (2007) argued that the high HONO mixing ratios during morning and late morning can be explained by mountain up-slope flow of polluted air from the cities at the foot of the mountain that results from ground surface heating. On Cyprus the sea breeze, driven by the growing difference between sea and soil surface temperature, brings air to the site which interacted with the soil surface and vegetation and is loaded by respective trace gas emissions. This is endorsed by the simultaneous increase of DMS and isoprene, markers for transportation of marine air and emission by vegetation. In the late afternoon, when the surface cools, down-welling air from aloft would dominate, being less influenced by ground surface processes. Zhou et al. (2007) could show that noontime HONO mixing ratios and average NO_y during the previous 24-hour period were strongly correlated, much better than instantaneous $HONO/NO_y$ or $HONO/NO_x$, which is in line with N-accumulation on soil surfaces as discussed above.

5.2 Daytime HONO budget

During daytime (7:30 to 18:00 LT, with HONO lifetime being between 10 and 30 min), $[HONO]_{PSS}$, the photostationary HONO concentration resulting from gas phase chemistry can be calculated according to Eq. (2) (Kleffmann et al., 2005):

$$[HONO]_{PSS} = \frac{k_1[OH][NO]}{k_2[OH]+J_{HONO}} \quad \text{(Eq.2)}$$

where k_1 and k_2 are the temperature dependent rate constants for the gas phase HONO formation from NO and OH and the loss of HONO by reaction of HONO and OH, respectively (Atkinson et al., 2004; e.g. at 23.0°C a typical temperature during this study $k_1 \approx 1.36 \times 10^{-11}$ $cm^3 s^{-1}$; $k_2 \approx 6.01 \times 10^{-12}$ $cm^3 s^{-1}$). J_{HONO} is the photolysis frequency of

HONO, which was measured with a spectroradiometer. [NO] is the observed NO concentration. Since OH data were available only on a few days, diel variations of [OH] were averaged (see fig. S3).

As has been previously established by many other studies (Su et al., 2008a; Michoud et al., 2014; Soergel et al., 2011a), homogeneous gas-phase chemistry alone fails to reflect observed HONO mixing ratios. Observed daytime values were up to 30 times higher than calculated based on PSS, indicating strong additional local daytime sources of HONO. Lee et al. (2013) argue that the HONO PSS assumption might overestimate the strength of any un-identified source, if the transport time from nearby NOx emission sources to the measurement site is less than the time required for HONO to reach PSS. In this study, the missing source was calculated according to Su et al., 2008a (eq.3), where PSS was not assumed. Also in our measurements, dHONO/dt was not equal to zero, as HONO was not at PSS.

$$S_{HONO} = J_{HONO}[HONO] + k_2[OH][HONO] - k_1[OH][NO] - k_{het}[NO_2] + \frac{\Delta[HONO]}{\Delta t} \quad \text{(Eq.3)}$$

with [HONO] being the measured HONO concentration and k_{het} the heterogeneous conversion rate of NO_2 to HONO, which was discussed above to be 1.6% h^{-1} during the wet period and 0.36% h^{-1} during the dry period. Δ[HONO]/Δt is the observed change of HONO concentration unequal to 0. The uncertainty of the calculated missing source S_{HONO} was estimated to be about 16% based on the Gaussian error propagation of instrument uncertainties of HONO, NO, NO_2, J and OH.

Nevertheless, at the study site of Cyprus, the mean upwind distance between the measurement site and the coast line was about 6 km, and the mean wind velocity was about 3 m s^{-1}. Accordingly, the respective air mass travel time over land is estimated to be about half an hour, which is somewhat longer than the daytime lifetime of HONO and might provide enough time for the equilibrium processes. Furthermore and in a strong contrast to Lee et al. (2013), at the Cyprus site the concentrations of HONO precursors (NO and OH) were extremely low, by far too low to explain the observed HONO concentrationsIn the late morning (around 10:00 LT) the unknown source was at its maximum with peak production rates of up to 3.4x10^6 molecules cm^{-3} s^{-1}, and a daytime average of about 1.3x10^6 cm^{-3} s^{-1}, which is in good agreement with other studies at rural sites like a mountain site at Hohenpeissenberg ((3±1)x10^6 cm^{-3} s^{-1}, at NO_x ≈ 2 ppbv, Acker et al., 2006a), a deciduous forest site in Jülich (3.45x10^6 molecules cm^{-3} s^{-1}, at NO ≈ 250 pptv, Kleffmann et al., 2005) and a pine forest site in South-West Spain 0.74x10^6 molecules cm^{-3} s^{-1}, at NO_x ≈1.5 ppbv, Soergel et al., 2011a) but smaller than at urban sites in Houston (4-6x10^6 cm^{-3} s^{-1}, at NO_x ≈ 6ppbv, Wong et al., 2012), Beijing (7x10^6 cm^{-3} s^{-1}, at NO_x ≈15 ppbv, Yang et al., 2014) and South China (5.25 ± 3.75x10^6 cm^{-3} s^{-1}, at NO_x ≈ 20 ppbv, Li et al., 2012; or 1-4x10^7 cm^{-3} s^{-1}, at NO_x ≈ 35 ppbv, Su et al., 2008a).

The contributions of gas phase reactions and the heterogeneous reaction of NO_2 (conversion rate (a) 1.6% h^{-1} and (b) 0.36% h^{-1}) to the HONO budget are illustrated in fig. 5, exemplary. For both periods the contributions are quiet similar just the absolute values are different. To compensate the strong loss via photolysis a comparable strong unknown source is necessary as the heterogeneous NO_2 conversion or the gasphase reaction of OH and NO are insignificant.

In polluted regions with moderate to high NO_x concentrations, HONO sources have often been linked with [NO_2] or [NO_x] (Acker et al., 2005, Li et al., 2012, Levy et al., 2014, Soergel et al., 2011a, Wentzel et al., 2010). Under the prevailing low NO_x conditions during CYPHEX (<250 pptv), correlation analysis (see table 1) of S_{HONO} with [NO_2] (R^2 = 0.50) and [NO_2]*RH (R^2 = 0.51) indicate no significant impact of instantaneous heterogeneous formation of

HONO from NO_2. Better correlations of S_{HONO} with J_{NO2} (R^2 = 0.67) and J_{NO2}*[NO_2] (R^2 = 0.82) indicate a photo-induced conversion of NO_2 to HONO as already suggested by George et al. (2005) or Stemmler et al. (2006, 2007). Lee et al. (2016) found even lower correlation with [NO_2] (R^2 = 0.0001) but similar good correlation with J_{NO2}*[NO_2] (R^2=0.70) at an urban background site in London. Other light dependent reactions such as the photolysis of nitrate might additionally contribute to high daytime HONO. It is unlikely that aerosol surfaces played an important role in heterogeneous conversion of NO_2 as the mean observed aerosol surface concentration was only about 300 μm^2 cm^{-3}. Based on a formula for photo enhanced conversion of NO_2 on humic acid aerosols which was derived by Stemmler et al. (2007) a HONO formation rate of only $5.1x10^2$ molecules cm^{-3} s^{-1} can be estimated. Likewise, Soergel et al. (2015) showed that HONO fluxes from light-activated reactions of NO_2 on humic acid surfaces at low NO_2 levels (< 1 ppb and thus comparable to concentrations observed in this study) saturated at around 0.0125 nmol m^{-2} s^{-1}. Therefore heterogeneous aerosol surface reactions can be neglected as HONO sources at the prevailing low NO_x levels.

Likewise, the nitrate concentrations of highly acidic marine aerosols particulate matter as measured by HR-ToF-AMS (PM1 fraction, mean 0.075 µg m^{-3}) were too low to account for significant photolytic HONO production ($1.7x10^2$ molecules cm^{-3} s^{-1} or 0.01% of S_{HONO}) calculated by Eq. (4):

$$S_{photo\_NO_3^-} = [\overline{NO_3^-}] \cdot J_{NO_3^-} \quad \text{(Eq. 4)}$$

with S_{photo_NO3-} the source strength of HONO by photolysis of nitrate, $[\overline{NO_3^-}]$ the mean particulate nitrate concentration and $J_{NO_3^-}$ the photolysis frequency of nitrate (aqueous) at noon ($3x10^{-7}$ s^{-1}, Jankowski et al., 1999).

Recently an enhancement of the photolysis frequency of particulate nitrate relative to gaseous or aqueous nitrate was found (Ye et al., 2016). But even with this enhanced rate of $2x10^{-4}$ s^{-1} not more than $1.1x10^5$ molecules cm^{-3} s^{-1} (8% of S_{HONO}) HONO would be produced.

5.3 Common daytime source of HONO and NO

During CYPHEX, good correlation was found between [HONO] or S_{HONO} and [NO] (R^2 = 0.86 and 0.60, respectively), indicating that both may have a common source. A missing source of NO can be calculated as shown in Eq. (5).

$$S_{NO} = k_1[OH][NO] + k_3[HO_2][NO] + k_4[O_3][NO] + k_5[RO_2][NO] - J_{NO2}[NO_2] - J_{HONO}[HONO] + \frac{\Delta[NO]}{\Delta t} \quad \text{(Eq. 5)}$$

k_3 and k_4 are the temperature dependent rate constants for the reaction of NO with HO_2 and O_3, respectively (Atkinson et al., 2004; at 23°C: $k_3 \approx 8.96x10^{-12}$ cm^3s^{-1}; $k_4 \approx 1.68x10^{-14}$ cm^3s^{-1}), k_5 is the rate constant for the reaction of NO and organic peroxy radicals which was assumed to be the same as for the reaction NO + CH_3O_2 ($7.7x10^{-12}$ cm^3s^{-1} at 298K, Ren et al., 2010; Sander et al., 2011). Like [OH] also [HO_2] was measured only on a few days and therefore mean diel data were used (fig. S3). Total [RO_2] was estimated to be maximum 1.6*[HO_2] (Ren et al., 2010; Hens et al., 2014). Using a RO_2/HO_2 ratio of 1.2 the absolute values of S_{NO} are reduced by 0.3 to 5.5%. The budget analysis for NO for both humidity regimes is illustrated in fig. S4.

For NO_x, an unexpected deviation from the PSS, or Leighton ratio, respectively, of clean marine boundary layer air has been observed previously, invoking a hitherto unknown NO sink, or pathway for NO to NO_2 oxidation, other than reactions with OH, HO_2, O_3 and organic peroxides (Beygi et al., 2011). On Cyprus, two different atmospheric humidity regimes can be differentiated. Under dry conditions (RH < 70%, yellow boxes in fig. 3) and higher NO_x concentrations (>150 pptv) S_{NO} is negative, implying a net NO sink of up to $6.4x10^7$ molecules cm^{-3} s^{-1} resembling the above mentioned PSS deviations in remote marine air masses (see fig. 6 and 7). However, during humid conditions (RH > 70, blue boxes in fig. 3) S_{NO} was positive with values of up to $5.1x10^7$ molecules cm^{-3} s^{-1}. Due to low and invariant acetonitrile levels, anthropogenic activity and local biomass burning can be excluded as NO source at this specific site. A net NO source during humid conditions is assumed to result from (biogenic) NO emission from soil. As shown in fig. 8, the S_{HONO} and S_{NO} (time of day-averaged, excluding 3 days as there are transition days 25.7. and 2.8. or the RH changed too quickly 15.7.) were highly correlated ($R^2 = 0.72$), indicative of both reactive N-compounds being emitted from the same local source. Both HONO and NO have been reported to be released from soil, with a strong dependency on soil water content (Su et al., 2011; Oswald et al., 2013; Mamtimin et al., 2016). The (dry state) soil humidification threshold level for NO emission is reported to be somewhat higher than for HONO (Oswald et al., 2013), which might explain why a net NO source was preferentially calculated for higher relative humidity conditions, while for HONO a daytime source under all humidity regimes prevailing during the campaign was found. Mamtimin et al. (2016) investigated HONO and NO emissions of natural desert soil and with grapes or cotton cultivated soils in an oasis in the Taklamakan desert in the Xinjiang region in China. After irrigation they didn´t find direct emission, but when the soil had almost dried out (gravimetric soil water content 0.01-0.3) emissions up to 115 ng N m^{-2} s^{-1} were detected. In addition they observed soil-temperature dependent emission of reactive nitrogen. Analyzing microbial surface communities from drylands, Weber et al. (2015) observed highly correlated NO-N and HONO-N emissions with Spearman rank correlation coefficients ranging between 0.75 and 0.99. In this study, NO- and HONO-emissions were observed in drying soils with water contents of 20-30% water holding capacity.

Even though we cannot make firm conclusions regarding the exact mechanism of HONO formation, the above mentioned correlation analysis (and table 1) reveal that the instantaneous heterogeneous NO_2 conversion is not a significant HONO source. We propose that HONO is emitted from nitrogen compounds being accumulated on mountain slope soil surfaces produced either biologically by soil microbiota or from previously deposited NO_y. This forms the major daytime HONO source responsible for morning concentration peaks and consistently high daytime mixing ratios at the Cyprus field site. While biological formation is assumed to be more relevant for humid conditions, physical NO_y accumulation can be assumed to be stronger under dry conditions, as uptake coefficients for a variety of trace gases were shown to be significantly higher for dry surfaces, among them NO_2 (Wang et al., 2012, Liu et al., 2015), HONO (Donaldson et al. 2014a) and HCHO (Li et al., 2016). The strongest HONO morning peaks observed after dry nights were accompanied by an increase in relative humidity driven by the sea breeze (fig. 4b), so we consider HONO being released preferentially under favourable humid conditions.

5.4 primary OH production

Many studies showed high contribution of HONO photolysis to the OH budget (up to 30% on daily average; Alicke et al., 2002, Ren et al., 2006). Here the primary OH production rates are calculated based on the main OH forming reactions, which are the photolysis of O_3 and subsequent reaction with water (R6+7), the photolysis of HONO (R2) and the reaction of alkenes with ozone (R8).

$$O_3 \xrightarrow{hv\ (<340\ nm)} O(^1D) + O_2 \quad \text{(R6)}$$

$$O(^1D) + H_2O \rightarrow 2\ OH \quad \text{(R7)}$$

$$\text{alkene} + O3 \rightarrow OH + \text{other products} \quad \text{(R8)}$$

Reaction rates were taken from Atkinson et al. (2004) and Atkinson (1997). The water pressure over water was calculated according to Murphy and Koop (2005). Reactions of $O(^1D)$ and HO_2 not forming OH are also considered. OH formation yields of the reactions of alkenes with O_3 were taken from Paulson et al. (1999). Photolysis rates (J-values) and concentrations of relevant compounds were as measured on Cyprus. Isoprene, α-pinene, β-pinene, Δ3-carene and limonene (VOC) were taken into account as the most relevant alkenes.

The results of this study are shown in fig. 9. All three production routes show a clear diel profile with higher production rates during daytime. In the night only the reaction of alkenes with O_3 produced significant amounts of OH ($2x10^4$ molecules cm^{-3} s^{-1}). With sunrise the other sources become more relevant. During day the photolysis of HONO generates about $1.5x10^6$ molecules OH cm^{-3} s^{-1}, which is about 10 times higher than the ozonolysis of alkenes at that time. The maximum OH production rate by O_3 photolysis during daytime is about $1.3x10^7$ molecules cm^{-3} s^{-1}. In the morning (6-8 am) and evening hours (7-8 pm) the contribution of HONO photolysis to the primary OH production is in average 37% (see fig. 9b) with peak values of 65%, which is much higher than the contribution of O_3 photolysis at that time. During the rest of the day the contribution of HONO decreases to 12%. At noon the most dominant OH source is the photolysis of O_3 (more than 80%) while the contribution of the ozonolysis of alkenes is almost negligible (1-2%). A complete and detailed HOx budget analysis with CYPHEX data will be published soon.

6 Conclusion

Nitrous acid was found in low concentrations on the east Mediterranean Island of Cyprus during summer 2014. Daytime concentrations were much higher than during the night and about 30 times higher than would be expected by budget analysis based on photostationary state. The unknown source was calculated to be about $1.9x10^6$ molecules cm^{-3} s^{-1} around noon. Low NO_x concentrations, high HONO/NO_x ratio and low correlation between HONO and NO_2 indicate a local source which is independent from NO_2. Heterogeneous reactions of NO_2 on aerosols play an insignificant role during daytime. Emission from soil, either caused by photolysis of nitrate or gas-soil partitioning of accumulated nitrite/nitrous acid, is supposed to have a higher impact on the HONO concentration during this campaign. Also the NO budget analysis showed a missing source in the humid period, which correlates well with the unknown source of HONO, indicating a common source. The most likely source of HONO and NO is the emission from soil.

Even though the HONO concentration is only in the lower pptv level, it has a high contribution to the primary OH production in the early morning and evening hours.

Acknowledgement

This study was supported by the Max Planck Society (MPG) and the DFG-Research Center / Cluster of Excellence „The Ocean in the Earth System-MARUM".

We thank the Cyprus Institute and the Department of Labor Inspection for the logistical support, as well as the military staff at the Lara Naval Observatory in Ineia for the excellent collaboration.

Furthermore we´d like to thank Mathias Soergel for his technical support on experimental set-up of atmospheric HONO measurements.

References

Acker, K., Moller, D., Auel, R., Wieprecht, W., and Kalass, D.: Concentrations of nitrous acid, nitric acid, nitrite and nitrate in the gas and aerosol phase at a site in the emission zone during ESCOMPTE 2001 experiment, Atmospheric Research, 74, 507-524, 2005.

Acker, K., Moller, D., Wieprecht, W., Meixner, F. X., Bohn, B., Gilge, S., Plass-Dulmer, C., and Berresheim, H.: Strong daytime production of OH from HNO2 at a rural mountain site, Geophysical Research Letters, 33, 2006a.

Acker, K., Febo, A., Trick, S., Perrino, C., Bruno, P., Wiesen, P., Moeller, D., Wieprecht, W., Auel, R., Giusto, M., Geyer, A., Platt, U., and Allegrini, I.: Nitrous acid in the urban area of Rome, Atmospheric Environment, 40, 3123-3133, 2006b.

Acker, K., Beysens, D., and Moeller, D.: Nitrite in dew, fog, cloud and rain water: An indicator for heterogeneous processes on surfaces, Atmospheric Research, 87, 200-212, 2008.

Alicke, B., Platt, U., and Stutz, J.: Impact of nitrous acid photolysis on the total hydroxyl radical budget during the Limitation of Oxidant Production/Pianura Padana Produzione di Ozono study in Milan, Journal of Geophysical Research-Atmospheres, 107, 2002.

Alicke, B., Geyer, A., Hofzumahaus, A., Holland, F., Konrad, S., Patz, H. W., Schafer, J., Stutz, J., Volz-Thomas, A., and Platt, U.: OH formation by HONO photolysis during the BERLIOZ experiment, Journal of Geophysical Research-Atmospheres, 108, 2003.Ammann, M., Kalberer, M., Jost, D. T., Tobler, L., Rossler, E., Piguet, D., Gaggeler, H. W., and Baltensperger, U.: Heterogeneous production of nitrous acid on soot in polluted air masses, Nature, 395, 157-160, 1998.

Amoroso, A., Domine, F., Esposito, G., Morin, S., Savarino, J., Nardino, M., Montagnoli, M., Bonneville, J. M., Clement, J. C., Ianniello, A., and Beine, H. J.: Microorganisms in Dry Polar Snow Are Involved in the Exchanges of Reactive Nitrogen Species with the Atmosphere, Environmental Science & Technology, 44, 714-719, 2010.

Arens, F., Gutzwiller, L., Baltensperger, U., Gaggeler, H. W., and Ammann, M.: Heterogeneous reaction of NO2 on diesel soot particles, Environmental Science & Technology, 35, 2191-2199, 2001.

Arey, J., Atkinson, R., and Aschmann, S. M.: Product study of the gas-phase reactions of monoterpenes with the OH radical in the presence of NOx, Journal of Geophysical Research: Atmospheres, 95, 18539-18546, 1990.

Atkinson, R.: Gas-Phase Tropospheric Chemistry of Volatile Organic Compounds: 1. Alkanes and Alkenes, Journal of Physical and Chemical Reference Data, 26, 215-290, 1997.

Atkinson, R., Baulch, D. L., Cox, R. A., Crowley, J. N., Hampson, R. F., Hynes, R. G., Jenkin, M. E., Rossi, M. J., and Troe, J.: Evaluated kinetic and photochemical data for atmospheric chemistry: Volume I - gas phase reactions of O-x, HOx, NOx and SOx species, Atmospheric Chemistry and Physics, 4, 1461-1738, 2004.

Aubin, D. G., and Abbatt, J. P. D.: Interaction of NO2 with hydrocarbon soot: Focus on HONO yield, surface modification, and mechanism, Journal of Physical Chemistry A, 111, 6263-6273, 2007.

Baergen, A. M., and Donaldson, D. J.: Photochemical Renoxification of Nitric Acid on Real Urban Grime, Environmental Science & Technology, 47, 815-820, 2013.

Beine, H. J., Allegrini, I., Sparapani, R., Ianniello, A., and Valentini, F.: Three years of springtime trace gas and particle measurements at Ny-Alesund, Svalbard, Atmospheric Environment, 35, 3645-3658, 2001.

Bejan, I., Abd El Aal, Y., Barnes, I., Benter, T., Bohn, B., Wiesen, P., and Kleffmann, J.: The photolysis of ortho-nitrophenols: a new gas phase source of HONO, Physical Chemistry Chemical Physics, 8, 2028-2035, 2006.

Beygi, Z. H., Fischer, H., Harder, H. D., Martinez, M., Sander, R., Williams, J., Brookes, D. M., Monks, P. S., and Lelieveld, J.: Oxidation photochemistry in the Southern Atlantic boundary layer: unexpected deviations of photochemical steady state, Atmospheric Chemistry and Physics, 11, 8497-8513, 2011.

Bianchi, M., Feliatra, F., Tréguer, P., Vincendeau, M.-A., and Morvan, J.: Nitrification rates, ammonium and nitrate distribution in upper layers of the water column and in sediments of the Indian sector of the Southern Ocean, Deep Sea Research Part II: Topical Studies in Oceanography, 44, 1017-1032, 1997.

Bohn, B., Corlett, G. K., Gillmann, M., Sanghavi, S., Stange, G., Tensing, E., Vrekoussis, M., Bloss, W. J., Clapp, L. J., Kortner, M., Dorn, H. P., Monks, P. S., Platt, U., Plass-Dulmer, C., Mihalopoulos, N., Heard, D. E., Clemitshaw, K. C., Meixner, F. X., Prevot, A. S. H., and Schmitt, R.: Photolysis frequency measurement techniques: results of a comparison within the ACCENT project, Atmospheric Chemistry and Physics, 8, 5373-5391, 2008.

Bröske, R., Kleffmann, J., and Wiesen, P.: Heterogeneous conversion of NO2 on secondary organic aerosol surfaces: A possible source of nitrous acid (HONO) in the atmosphere?, Atmospheric Chemistry and Physics, 3, 469-474, 2003.

Costabile, F., Amoroso, A., and Wang, F.: Sub-mu m particle size distributions in a suburban Mediterranean area. Aerosol populations and their possible relationship with HONO mixing ratios, Atmospheric Environment, 44, 5258-5268, 2010.

Czader, B. H., Rappenglueck, B., Percell, P., Byun, D. W., Ngan, F., and Kim, S.: Modeling nitrous acid and its impact on ozone and hydroxyl radical during the Texas Air Quality Study 2006, Atmospheric Chemistry and Physics, 12, 6939-6951, 2012.

Donaldson, M. A., Berke, A. E., and Raff, J. D.: Uptake of Gas Phase Nitrous Acid onto Boundary Layer Soil Surfaces, Environmental Science & Technology, 48, 375-383, 2014a.

Donaldson, M. A., Bish, D. L., and Raff, J. D.: Soil surface acidity plays a determining role in the atmospheric-terrestrial exchange of nitrous acid, Proceedings of the National Academy of Sciences, 111, 18472-18477, 2014b.

Duplissy, J., Gysel, M., Alfarra, M. R., Dommen, J., Metzger, A., Prevot, A. S. H., Weingartner, E., Laaksonen, A., Raatikainen, T., Good, N., Turner, S. F., McFiggans, G., and Baltensperger, U.: Cloud forming potential of secondary organic aerosol under near atmospheric conditions, Geophysical Research Letters, 35, 2008.

Elshorbany, Y. F., Steil, B., Brühl, C., and Lelieveld, J.: Impact of HONO on global atmospheric chemistry calculated with an empirical parameterization in the EMAC model, Atmospehric Chemistry and Physics, 12, 9977-10000, 2012.

Finlayson-Pitts, B. J., Wingen, L. M., Sumner, A. L., Syomin, D., and Ramazan, K. A.: The heterogeneous hydrolysis of NO2 in laboratory systems and in outdoor and indoor atmospheres: An integrated mechanism, Physical Chemistry Chemical Physics, 5, 223-242, 2003.

Foster, J. R., Pribush, R. A., and Carter, B. H.: THE CHEMISTRY OF DEWS AND FROSTS IN INDIANAPOLIS, INDIANA, Atmospheric Environment Part a-General Topics, 24, 2229-2236, 1990.

George, C., Strekowski, R. S., Kleffmann, J., Stemmler, K., and Ammann, M.: Photoenhanced uptake of gaseous NO2 on solid-organic compounds: a photochemical source of HONO?, Faraday Discussions, 130, 195-210, 2005.

Han, C., Liu, Y., and He, H.: Role of Organic Carbon in Heterogeneous Reaction of NO2 with Soot, Environmental science & technology, 47, 3174-3181, 2013.

Harrison, R. M., and Kitto, A. M. N.: EVIDENCE FOR A SURFACE SOURCE OF ATMOSPHERIC NITROUS-ACID, Atmospheric Environment, 28, 1089-1094, 1994.

He, Y., Zhou, X. L., Hou, J., Gao, H. L., and Bertman, S. B.: Importance of dew in controlling the air-surface exchange of HONO in rural forested environments, Geophysical Research Letters, 33, 2006.

Heland, J., Kleffmann, J., Kurtenbach, R., and Wiesen, P.: A new instrument to measure gaseous nitrous acid (HONO) in the atmosphere, Environmental Science & Technology, 35, 3207-3212, 2001.

Hens, K., Novelli, A., Martinez, M., Auld, J., Axinte, R., Bohn, B., Fischer, H., Keronen, P., Kubistin, D., Noelscher, A. C., Oswald, R., Paasonen, P., Petaja, T., Regelin, E., Sander, R., Sinha, V., Sipila, M., Taraborrelli, D., Ernest, C. T., Williams, J., Lelieveld, J., and Harder, H.: Observation and modelling of HOx radicals in a boreal forest, Atmospheric Chemistry and Physics, 14, 8723-8747, 2014.

Huang, G., Zhou, X. L., Deng, G. H., Qiao, H. C., and Civerolo, K.: Measurements of atmospheric nitrous acid and nitric acid, Atmospheric Environment, 36, 2225-2235, 2002.

IUPAC: Task Group on Atmospheric Chemical Kinetic Data Evaluation, (Ammann, M., Cox, R.A., Crowley, J.N., Jenkin, M.E., Mellouki, A., Rossi, M. J., Troe, J. and Wallington, T. J.) http://iupac.pole-ether.fr/index.html., 2015.

Jacobi, H. W., Bales, R. C., Honrath, R. E., Peterson, M. C., Dibb, J. E., Swanson, A. L., and Albert, M. R.: Reactive trace gases measured in the interstitial air of surface snow at Summit, Greenland, Atmospheric Environment, 38, 1687-1697, 2004.

Jankowski, J. J., Kieber, D. J., and Mopper, K.: Nitrate and nitrite ultraviolet actinometers, Photochemistry and Photobiology, 70, 319-328, 1999.

Jiang, Q. Q., and Bakken, L. R.: Comparison of Nitrosospira strains isolated from terrestrial environments, FEMS Microbiology Ecology, 30, 171-186, 1999.

Kalberer, M., Ammann, M., Arens, F., Gaggeler, H. W., and Baltensperger, U.: Heterogeneous formation of nitrous acid (HONO) on soot aerosol particles, Journal of Geophysical Research-Atmospheres, 104, 13825-13832, 1999.

Kebede, M. A., Scharko, N. K., Appelt, L. E., and Raff, J. D.: Formation of Nitrous Acid during Ammonia Photooxidation on TiO2 under Atmospherically Relevant Conditions, Journal of Physical Chemistry Letters, 4, 2618-2623, 2013.

Kerbrat, M., Legrand, M., Preunkert, S., Gallée, H., and Kleffmann, J.: Nitrous acid at Concordia (inland site) and Dumont d'Urville (coastal site), East Antarctica, Journal of Geophysical Research: Atmospheres, 117, D08303, 2012.

Kessler, C., and Platt, U.: Nitrous Acid in Polluted Air Masses — Sources and Formation Pathways, in: Physico-Chemical Behaviour of Atmospheric Pollutants, edited by: Versino, B., and Angeletti, G., Springer Netherlands, 412-422, 1984.

Kinugawa, T., Enami, S., Yabushita, A., Kawasaki, M., Hoffmann, M. R., and Colussi, A. J.: Conversion of gaseous nitrogen dioxide to nitrate and nitrite on aqueous surfactants, Physical Chemistry Chemical Physics, 13, 5144-5149, 2011.

Khlystov, A., Stanier, C., and Pandis, S. N.: An algorithm for combining electrical mobility and aerodynamic size distributions data when measuring ambient aerosol, Aerosol Science and Technology, 38, 229-238, 2004.

Kleanthous, S., Vrekoussis, M., Mihalopoulos, N., Kalabokas, P., and Lelieveld, J.: On the temporal and spatial variation of ozone in Cyprus, Science of The Total Environment, 476–477, 677-687, 2014.

Kleffmann, J., Becker, K. H., and Wiesen, P.: Heterogeneous NO2 conversion processes on acid surfaces: possible atmospheric implications, Atmospheric Environment, 32, 2721-2729, 1998.

Kleffmann, J., H. Becker, K., Lackhoff, M., and Wiesen, P.: Heterogeneous conversion of NO2 on carbonaceous surfaces, Physical Chemistry Chemical Physics, 1, 5443-5450, 1999.

Kleffmann, J., Kurtenbach, R., Lorzer, J., Wiesen, P., Kalthoff, N., Vogel, B., and Vogel, H.: Measured and simulated vertical profiles of nitrous acid - Part I: Field measurements, Atmospheric Environment, 37, 2949-2955, 2003.

Kleffmann, J., Gavriloaiei, T., Hofzumahaus, A., Holland, F., Koppmann, R., Rupp, L., Schlosser, E., Siese, M., and Wahner, A.: Daytime formation of nitrous acid: A major source of OH radicals in a forest, Geophysical Research Letters, 32, 2005.

Kleffmann, J., and Wiesen, P.: Heterogeneous conversion of NO2 and NO on HNO3 treated soot surfaces: atmospheric implications, Atmospheric Chemistry and Physics, 5, 77-83, 2005.

Kurtenbach, R., Becker, K. H., Gomes, J. A. G., Kleffmann, J., Lorzer, J. C., Spittler, M., Wiesen, P., Ackermann, R., Geyer, A., and Platt, U.: Investigations of emissions and heterogeneous formation of HONO in a road traffic tunnel, Atmospheric Environment, 35, 3385-3394, 2001.

Lammel, G., and Cape, J. N.: Nitrous acid and nitrite in the atmosphere, Chemical Society Reviews, 25, 361-369, 1996.

Langridge, J. M., Gustafsson, R. J., Griffiths, P. T., Cox, R. A., Lambert, R. M., and Jones, R. L.: Solar driven nitrous acid formation on building material surfaces containing titanium dioxide: A concern for air quality in urban areas?, Atmospheric Environment, 43, 5128-5131, 2009.

Lee, B. H., Wood, E. C., Herndon, S. C., Lefer, B. L., Luke, W. T., Brune, W. H., Nelson, D. D., Zahniser, M. S., and Munger, J. W.: Urban measurements of atmospheric nitrous acid: A caveat on the interpretation of the HONO photostationary state, J. Geophys. Res., vol. 118, 12274–12281, 2013.

Lee, J. D., Whalley, L. K., Heard, D. E., Stone, D., Dunmore, R. E., Hamilton, J. F., Young, D. E., Allan, J. D., Laufs, S., and Kleffmann, J.: Detailed budget analysis of HONO in central London reveals a missing daytime source, Atmospheric Chemistry and Physics, 16, 2747-2764, 2016.

Legrand, M., Preunkert, S., Frey, M., Bartels-Rausch, T., Kukui, A., King, M. D., Savarino, J., Kerbrat, M., and Jourdain, B.: Large mixing ratios of atmospheric nitrous acid (HONO) at Concordia (East Antarctic Plateau) in summer: a strong source from surface snow?, Atmospheric Chemistry and Physics, 14, 9963-9976, 2014.

Lelièvre, S., Bedjanian, Y., Laverdet, G., and Le Bras, G.: Heterogeneous Reaction of NO2 with Hydrocarbon Flame Soot, The Journal of Physical Chemistry A, 108, 10807-10817, 2004.

Levy, H.: Normal Atmosphere: Large Radical and Formaldehyde Concentrations Predicted, Science, 173, 141-143, 1971.

Levy, M., Zhang, R., Zheng, J., Zhang, A. L., Xu, W., Gomez-Hernandez, M., Wang, Y., and Olaguer, E.: Measurements of nitrous acid (HONO) using ion drift-chemical ionization mass spectrometry during the 2009 SHARP field campaign, Atmospheric Environment, 94, 231-240, 2014.

Li, J., A. Reiffs, U. Parchatka, and H. Fischer, In situ measurements of atmospheric CO and its correlation with NO_x and O_3 at a rural mountain site, *Metrol.Meas. Syst.*, XXII, 25-38, 2015.

Li, S. M.: Equilibrium of particle nitrite with gas-phase HONO – tropospheric measurements in the high arctic during sunrise, Journal of Geophysical Research-Atmospheres, 99, 25469-25478, 1994.

Li, X., Brauers, T., Haeseler, R., Bohn, B., Fuchs, H., Hofzumahaus, A., Holland, F., Lou, S., Lu, K. D., Rohrer, F., Hu, M., Zeng, L. M., Zhang, Y. H., Garland, R. M., Su, H., Nowak, A., Wiedensohler, A., Takegawa, N., Shao, M., and Wahner, A.: Exploring the atmospheric chemistry of nitrous acid (HONO) at a rural site in Southern China, Atmospheric Chemistry and Physics, 12, 1497-1513, 2012.

Li, G., Su, H., Li, X., Kuhn, U., Meusel, H., Hoffmann, T., Ammann, M., Pöschl, U., Shao, M., and Cheng, Y.: Uptake of gaseous formaldehyde by soil surfaces: a combination of adsorption/desorption equilibrium and chemical reactions, Atmospheric Chemistry and Physics ,16, 10299-10311, 2016.

Liao, W., Case, A. T., Mastromarino, J., Tan, D., and Dibb, J. E.: Observations of HONO by laser-induced fluorescence at the South Pole during ANTCI 2003, Geophysical Research Letters, 33, L09810, 2006.

Liu, Y., Han, C., Ma, J., Bao, X., and He, H.: Influence of relative humidity on heterogeneous kinetics of NO2 on kaolin and hematite, Physical Chemistry Chemical Physics, 17, 19424-19431, 2015.

Mamtimin, B., Meixner, F. X., Behrendt, T., Badawy, M., and Wagner, T.: The contribution of soil biogenic NO and HONO emissions from a managed hyperarid ecosystem to the regional NOx emissions during growing season, Atmospheric Chemistry and Physics., 16, 10175-10194, 2016.

Mao, J., Ren, X., Chen, S., Brune, W. H., Chen, Z., Martinez, M., Harder, H., Lefer, B., Rappenglück, B., Flynn, J., and Leuchner, M.: Atmospheric oxidation capacity in the summer of Houston 2006: Comparison with summer measurements in other metropolitan studies, Atmospheric Environment, 44, 4107-4115, 2010.

Martinez, M., Harder, H., Kubistin, D., Rudolf, M., Bozem, H., Eerdekens, G., Fischer, H., Kluepfel, T., Gurk, C., Koenigstedt, R., Parchatka, U., Schiller, C. L., Stickler, A., Williams, J., and Lelieveld, J.: Hydroxyl radicals in the tropical troposphere over the Suriname rainforest: airborne measurements, Atmospheric Chemistry and Physics, 10, 3759-3773, 2010.

Michoud, V., Colomb, A., Borbon, A., Miet, K., Beekmann, M., Camredon, M., Aumont, B., Perrier, S., Zapf, P., Siour, G., Ait-Helal, W., Afif, C., Kukui, A., Furger, M., Dupont, J. C., Haeffelin, M., and Doussin, J. F.: Study of the unknown HONO daytime source at a European suburban site during the MEGAPOLI summer and winter field campaigns, Atmospheric Chemistry and Physics, 14, 2805-2822, 2014.

Monge, M. E., D'Anna, B., Mazri, L., Giroir-Fendler, A., Ammann, M., Donaldson, D. J., and George, C.: Light changes the atmospheric reactivity of soot, Proceedings of the National Academy of Sciences of the United States of America, 107, 6605-6609, 2010.

Murphy, D. M., and Koop, T.: Review of the vapour pressures of ice and supercooled water for atmospheric applications, Quarterly Journal of the Royal Meteorological Society, 131, 1539-1565, 10.1256/qj.04.94, 2005.

Ndour, M., D'Anna, B., George, C., Ka, O., Balkanski, Y., Kleffmann, J., Stemmler, K., and Ammann, M.: Photoenhanced uptake of NO2 on mineral dust: Laboratory experiments and model simulations, Geophysical Research Letters, 35, 2008.

Novelli, A., Hens, K., Ernest, C. T., Kubistin, D., Regelin, E., Elste, T., Plass-Dulmer, C., Martinez, M., Lelieveld, J., and Harder, H.: Characterisation of an inlet pre-injector laser-induced fluorescence instrument for the measurement of atmospheric hydroxyl radicals, Atmospheric Measurement Techniques, 7, 3413-3430.

Oswald, R., Behrendt, T., Ermel, M., Wu, D., Su, H., Cheng, Y., Breuninger, C., Moravek, A., Mougin, E., Delon, C., Loubet, B., Pommerening-Roeser, A., Soergel, M., Poeschl, U., Hoffmann, T., Andreae, M. O., Meixner, F. X., and Trebs, I.: HONO Emissions from Soil Bacteria as a Major Source of Atmospheric Reactive Nitrogen, Science, 341, 1233-1235, 2013.

Oswald, R., Ermel, M., Hens, K., Novelli, A., Ouwersloot, H. G., Paasonen, P., Petaja, T., Sipila, M., Keronen, P., Back, J., Konigstedt, R., Beygi, Z. H., Fischer, H., Bohn, B., Kubistin, D., Harder, H., Martinez, M., Williams, J., Hoffmann, T., Trebs, I., and Soergel, M.: A comparison of HONO budgets for two measurement heights at a field station within the boreal forest in Finland, Atmospheric Chemistry and Physics, 15, 799-813, 2015.

Paulson, S. E., Chung, M. Y., and Hasson, A. S.: OH radical formation from the gas-phase reaction of ozone with terminal alkenes and the relationship between structure and mechanism, Journal of Physical Chemistry A, 103, 8125-8138, 1999.

Pikridas, M., Bougiatioti, A., Hildebrandt, L., Engelhart, G. J., Kostenidou, E., Mohr, C., Prévôt, A. S. H., Kouvarakis, G., Zarmpas, P., Burkhart, J. F., Lee, B. H., Psichoudaki, M., Mihalopoulos, N., Pilinis, C., Stohl, A., Baltensperger, U., Kulmala, M., and Pandis, S. N.: The Finokalia Aerosol Measurement Experiment – 2008 (FAME-08): an overview, Atmospheric Chemistry and Physics, 10, 6793-6806, 2010.

Pitts, J. N., Sanhueza, E., Atkinson, R., Carter, W. P. L., Winer, A. M., Harris, G. W., and Plum, C. N.: An investigation of the dark formation of nitrous acid in environmental chambers, International Journal of Chemical Kinetics, 16, 919-939, 1984.

Quastel, J. H.: Soil Metabolism, Annual Review of Plant Physiology, 16, 217-240, 1965.

Ramazan, K. A., Syomin, D., and Finlayson-Pitts, B. J.: The photochemical production of HONO during the heterogeneous hydrolysis of NO2, Physical Chemistry Chemical Physics, 6, 3836-3843, 2004.

Ren, X. R., Harder, H., Martinez, M., Lesher, R. L., Oliger, A., Simpas, J. B., Brune, W. H., Schwab, J. J., Demerjian, K. L., He, Y., Zhou, X. L., and Gao, H. G.: OH and HO2 chemistry in the urban atmosphere of New York City, Atmospheric Environment, 37, 3639-3651, 2003.

Ren, X., Brune, W. H., Oliger, A., Metcalf, A. R., Simpas, J. B., Shirley, T., Schwab, J. J., Bai, C., Roychowdhury, U., Li, Y., Cai, C., Demerjian, K. L., He, Y., Zhou, X., Gao, H., and Hou, J.: OH, HO2, and OH reactivity during the PMTACS-NY Whiteface Mountain 2002 campaign: Observations and model comparison, Journal of Geophysical Research-Atmospheres, 111, 2006.

Ren, X., Gao, H., Zhou, X., Crounse, J. D., Wennberg, P. O., Browne, E. C., LaFranchi, B. W., Cohen, R. C., McKay, M., Goldstein, A. H., and Mao, J.: Measurement of atmospheric nitrous acid at Blodgett Forest during BEARPEX2007, Atmospheric Chemistry and Physics, 10, 6283-6294, 2010.

Ren, X., Sanders, J. E., Rajendran, A., Weber, R. J., Goldstein, A. H., Pusede, S. E., Browne, E. C., Min, K. E., and Cohen, R. C.: A relaxed eddy accumulation system for measuring vertical fluxes of nitrous acid, Atmospheric Measurement Techniques, 4, 2093-2103, 2011.

Rubio, M. A., Lissi, E., and Villena, G.: Nitrite in rain and dew in Santiago city, Chile. Its possible impact on the early morning start of the photochemical smog, Atmospheric Environment, 36, 293-297, 2002.

Sander, S. P., J. Abbatt, J. R. Barker, J. B. Burkholder, R. R. Friedl, D. M. Golden, R. E. Huie, C. E. Kolb, M. J. Kurylo, G. K. Moortgat, V. L. Orkin. and P. H. Wine: Chemical Kinetics and Photochemical Data for Use in Atmospheric Studies, Evaluation No. 17, JPL Publication 10-6, Jet Propulsion Laboratory, Pasadena, 2011, http://jpldataeval.jpl.nasa.gov.

Scharko, N. K., Berke, A. E., and Raff, J. D.: Release of Nitrous Acid and Nitrogen Dioxide from Nitrate Photolysis in Acidic Aqueous Solutions, Environmental Science & Technology, 48, 11991-12001, 2014.

Soergel, M., Regelin, E., Bozem, H., Diesch, J. M., Drewnick, F., Fischer, H., Harder, H., Held, A., Hosaynali-Beygi, Z., Martinez, M., and Zetzsch, C.: Quantification of the unknown HONO daytime source and its relation to NO2, Atmospheric Chemistry and Physics, 11, 10433-10447, 2011a.

Soergel, M., Trebs, I., Serafimovich, A., Moravek, A., Held, A., and Zetzsch, C.: Simultaneous HONO measurements in and above a forest canopy: influence of turbulent exchange on mixing ratio differences, Atmospheric Chemistry and Physics, 11, 841-855, 2011b.

Spataro, F., Ianniello, A., Esposito, G., Allegrini, I., Zhu, T., and Hu, M.: Occurrence of atmospheric nitrous acid in the urban area of Beijing (China), The Science of the total environment, 447, 210-224, 2013.

Stemmler, K., Ammann, M., Donders, C., Kleffmann, J., and George, C.: Photosensitized reduction of nitrogen dioxide on humic acid as a source of nitrous acid, Nature, 440, 195-198, 2006.

Stemmler, K., Ndour, M., Elshorbany, Y., Kleffmann, J., D'Anna, B., George, C., Bohn, B., and Ammann, M.: Light induced conversion of nitrogen dioxide into nitrous acid on submicron humic acid aerosol, Atmospheric Chemistry and Physics, 7, 4237-4248, 2007.

Stutz, J., Alicke, B., and Neftel, A.: Nitrous acid formation in the urban atmosphere: Gradient measurements of NO2 and HONO over grass in Milan, Italy, Journal of Geophysical Research-Atmospheres, 107, 2002.

Su, H., Cheng, Y. F., Shao, M., Gao, D. F., Yu, Z. Y., Zeng, L. M., Slanina, J., Zhang, Y. H., and Wiedensohler, A.: Nitrous acid (HONO) and its daytime sources at a rural site during the 2004 PRIDE-PRD experiment in China, Journal of Geophysical Research-Atmospheres, 113, 2008a.

Su, H., Cheng, Y. F., Cheng, P., Zhang, Y. H., Dong, S., Zeng, L. M., Wang, X., Slanina, J., Shao, M., and Wiedensohler, A.: Observation of nighttime nitrous acid (HONO) formation at a non-urban site during PRIDE-PRD2004 in China, Atmospheric Environment, 42, 6219-6232, 2008b.

Su, H., Cheng, Y., Oswald, R., Behrendt, T., Trebs, I., Meixner, F. X., Andreae, M. O., Cheng, P., Zhang, Y., and Poeschl, U.: Soil Nitrite as a Source of Atmospheric HONO and OH Radicals, Science, 333, 1616-1618, 2011.

Tang, Y., An, J., Wang, F., Li, Y., Qu, Y., Chen, Y., and Lin, J.: Impacts of an unknown daytime HONO source on the mixing ratio and budget of HONO, and hydroxyl, hydroperoxyl, and organic peroxy radicals, in the coastal regions of China, Atmospheric Chemistry and Physics, 15, 9381-9398, 2015.

VandenBoer, T. C., Brown, S. S., Murphy, J. G., Keene, W. C., Young, C. J., Pszenny, A. A. P., Kim, S., Warneke, C., de Gouw, J. A., Maben, J. R., Wagner, N. L., Riedel, T. P., Thornton, J. A., Wolfe, D. E., Dubé, W. P., Öztürk, F., Brock, C. A., Grossberg, N., Lefer, B., Lerner, B., Middlebrook, A. M., and Roberts, J. M.: Understanding the role of the ground surface in HONO vertical structure: High resolution vertical profiles during NACHTT-11, Journal of Geophysical Research: Atmospheres, 118, 10,155-110,171, 2013.

VandenBoer, T. C., Markovic, M. Z., Sanders, J. E., Ren, X., Pusede, S. E., Browne, E. C., Cohen, R. C., Zhang, L., Thomas, J., Brune, W. H., and Murphy, J. G.: Evidence for a nitrous acid (HONO) reservoir at the ground surface in Bakersfield, CA, during CalNex 2010, Journal of Geophysical Research-Atmospheres, 119, 9093-9106, 2014.

VandenBoer, T. C., Young, C. J., Talukdar, R. K., Markovic, M. Z., Brown, S. S., Roberts, J. M., and Murphy, J. G.: Nocturnal loss and daytime source of nitrous acid through reactive uptake and displacement, Nature Geosci, 8, 55-60, 2015.

Villena, G., Kleffmann, J., Kurtenbach, R., Wiesen, P., Lissi, E., Rubio, M. A., Croxatto, G., and Rappenglueck, B.: Vertical gradients of HONO, NOx and O-3 in Santiago de Chile, Atmospheric Environment, 45, 3867-3873, 2011.

Vogel, B., Vogel, H., Kleffmann, J., and Kurtenbach, R.: Measured and simulated vertical profiles of nitrous acid - Part II. Model simulations and indications for a photolytic source, Atmospheric Environment, 37, 2957-2966, 2003.

Wang, S. H., Ackermann, R., Spicer, C. W., Fast, J. D., Schmeling, M., and Stutz, J.: Atmospheric observations of enhanced NO2-HONO conversion on mineral dust particles, Geophysical Research Letters, 30, 2003.

Wang, L., Wang, W., and Ge, M.: Heterogeneous uptake of NO2 on soils under variable temperature and relative humidity conditions, Journal of Environmental Sciences, 24, 1759-1766, 2012.

Weber, B., Wu, D., Tamm, A., Ruckteschler, N., Rodriguez-Caballero, E., Steinkamp, J., Meusel, H., Elbert, W., Behrendt, T., Soergel, M., Cheng, Y., Crutzen, P. J., Su, H., and Poeschi, U.: Biological soil crusts accelerate the nitrogen cycle through large NO and HONO emissions in drylands, Proceedings of the National Academy of Sciences of the United States of America, 112, 15384-15389, 2015.

Wentzell, J. J. B., Schiller, C. L., and Harris, G. W.: Measurements of HONO during BAQS-Met, Atmospheric Chemistry and Physics, 10, 12285-12293, 2010.

Wong, K. W., Tsai, C., Lefer, B., Haman, C., Grossberg, N., Brune, W. H., Ren, X., Luke, W., and Stutz, J.: Daytime HONO vertical gradients during SHARP 2009 in Houston, TX, Atmospheric Chemistry and Physics, 12, 635-652, 2012.

Wong, K. W., Tsai, C., Lefer, B., Grossberg, N., and Stutz, J.: Modeling of daytime HONO vertical gradients during SHARP 2009, Atmospheric Chemistry and Physics, 13, 3587-3601, 2013.

Yabushita, A., Enami, S., Sakamoto, Y., Kawasaki, M., Hoffmann, M. R., and Colussi, A. J.: Anion-Catalyzed Dissolution of NO2 on Aqueous Microdroplets, The Journal of Physical Chemistry A, 113, 4844-4848, 2009.

Yang, Q., Su, H., Li, X., Cheng, Y., Lu, K., Cheng, P., Gu, J., Guo, S., Hu, M., Zeng, L., Zhu, T., and Zhang, Y.: Daytime HONO formation in the suburban area of the megacity Beijing, China, Science China Chemistry, 57, 1032-1042, 2014.

Ye, C., Zhou, X., Pu, D., Stutz, J., Festa, J., Spolaor, M., Tsai, C., Cantrell, C., Mauldin, R. L., Campos, T., Weinheimer, A., Hornbrook, R. S., Apel, E. C., Guenther, A., Kaser, L., Yuan, B., Karl, T., Haggerty, J., Hall, S., Ullmann, K., Smith, J. N., Ortega, J., and Knote, C.: Rapid cycling of reactive nitrogen in the marine boundary layer, Nature, 532, 489-491, 2016.

Young, C. J., Washenfelder, R. A., Roberts, J. M., Mielke, L. H., Osthoff, H. D., Tsai, C., Pikelnaya, O., Stutz, J., Veres, P. R., Cochran, A. K., VandenBoer, T. C., Flynn, J., Grossberg, N., Haman, C. L., Lefer, B., Stark, H., Graus, M., de Gouw, J., Gilman, J. B., Kuster, W. C., and Brown, S. S.: Vertically Resolved Measurements of Nighttime Radical Reservoirs; in Los Angeles and Their Contribution to the Urban Radical Budget, Environmental Science & Technology, 46, 10965-10973, 2012.

Zhang, N., Zhou, X. L., Shepson, P. B., Gao, H. L., Alaghmand, M., and Stirm, B.: Aircraft measurement of HONO vertical profiles over a forested region, Geophysical Research Letters, 36, 2009.

Zhou, X. L., Beine, H. J., Honrath, R. E., Fuentes, J. D., Simpson, W., Shepson, P. B., and Bottenheim, J. W.: Snowpack photochemical production of HONO: a major source of OH in the Arctic boundary layer in springtime, Geophysical Research Letters, 28, 4087-4090, 2001.

Zhou, X. L., Civerolo, K., Dai, H. P., Huang, G., Schwab, J., and Demerjian, K.: Summertime nitrous acid chemistry in the atmospheric boundary layer at a rural site in New York State, Journal of Geophysical Research-Atmospheres, 107, 2002a.

Zhou, X. L., He, Y., Huang, G., Thornberry, T. D., Carroll, M. A., and Bertman, S. B.: Photochemical production of nitrous acid on glass sample manifold surface, Geophysical Research Letters, 29, 2002b.

Zhou, X. L., Gao, H. L., He, Y., Huang, G., Bertman, S. B., Civerolo, K., and Schwab, J.: Nitric acid photolysis on surfaces in low-NOx environments: Significant atmospheric implications, Geophysical Research Letters, 30, 2003.

Zhou, X., Huang, G., Civerolo, K., Roychowdhury, U., and Demerjian, K. L.: Summertime observations of HONO, HCHO, and O-3 at the summit of Whiteface Mountain, New York, Journal of Geophysical Research-Atmospheres, 112, 2007.

Zhou, X., Zhang, N., TerAvest, M., Tang, D., Hou, J., Bertman, S., Alaghmand, M., Shepson, P. B., Carroll, M. A., Griffith, S., Dusanter, S., and Stevens, P. S.: Nitric acid photolysis on forest canopy surface as a source for tropospheric nitrous acid, Nature Geoscience, 4, 440-443, 2011.

Zhou, Y., Rosen, E. P., Zhang, H., Rattanavaraha, W., Wang, W., and Kamens, R. M.: SO2 oxidation and nucleation studies at near-atmospheric conditions in outdoor smog chamber, Environmental Chemistry, 10, 210-220, 2013.

Table 1: Linear correlation factors (Pearson correlation, R^2) of HONO and the unknown source S_{HONO} to meteorological factors and different NO_x parameters.

	during the whole campaign			
			Time of day average	
	HONO	S_{HONO}	HONO	S_{HONO}
T	0.006	0.125	0.488	0.214
RH	0.077	0.005*	0.092	0.103
Heat flux	0.261	0.300	0.617[c]	0.585[c]
J_{NO2}	0.263	0.395	**0.718[b]**	**0.672[b]**
NO	0.242	0.154	**0.857[a]**	0.600[c]
NO_2	0.052	0.078	0.620[c]	0.496
NO_2*RH	0.126	0.111	0.638[c]	0.505[c]
NO_2*RH*aerosol surface	0.095	0.092	0.256	0.579[c]
NO_2*J	0.191	0.164	**0.828[a]**	**0.813[a]**
NO_2*RH*J	0.266	0.221	**0.850[a]**	**0.807[a]**
NO_2*RH*J*aerosol surface	0.221	0.204	**0.806[a]**	**0.814[a]**
S_{NO}		0.012		-0.015*

a	highly correlated $R^2 > 0.8$
b	moderate correlated $R^2 > 0.65$
c	poorly correlated $R^2 > 0.5$
*	anti-correlated

	during the humid period				during the dry period			
			Time of day average				Time of day average	
	HONO	S_{HONO}	HONO	S_{HONO}	HONO	S_{HONO}	HONO	S_{HONO}
T	0.006	0.116	0.031	0.123	0.120	0.016	0.453	-0.004
RH	0.000	0.081*	0.010*	0.146*	0.374	0.193	**0.730[b]**	0.603[c]
Heat flux	0.110	0.243	0.184	0.591[c]	0.502[c]	0.335	**0.685[b]**	0.634[c]
J_{NO2}	0.150	0.465	0.245	**0.669[b]**	**0.678[b]**	0.320	**0.829[a]**	**0.664[b]**
NO	0.168	0.135	0.418	**0.650[b]**	0.487	0.301	**0.730[b]**	0.409
NO_2	0.066	0.065	0.300	0.267	0.037	0.003*	0.619[c]	0.174
NO_2*RH	0.084	0.048	0.294	0.171	0.161	0.010	**0.714[b]**	0.456
NO_2*RH*aerosol surface	0.047	0.072	0.111	0.250	0.241	0.085	0.557[c]	0.551[c]
NO_2*J	0.214	0.261	0.427	**0.845[a]**	0.358	0.016	**0.872[a]**	**0.603[b]**
NO_2*RH*J	0.231	0.244	0.467	**0.775[b]**	0.434	0.068	**0.820[a]**	**0.703[b]**
NO_2*RH*J*aerosol surface	0.140	0.152	0.465	**0.795[b]**	0.414	0.130	**0.664[b]**	0.631[c]
S_{NO}		0.294		**0.720[b]**		0.059		0.094

Figure 1: Map of location: the red star shows the location of Ineia and the measuring site. The four red points mark the main cities of Cyprus, Nicosia, Larnaca, Limassol and Paphos (clockwise ordering), map produced by the Cartographic Research Lab University of Alabama, map of Cyprus: google maps.

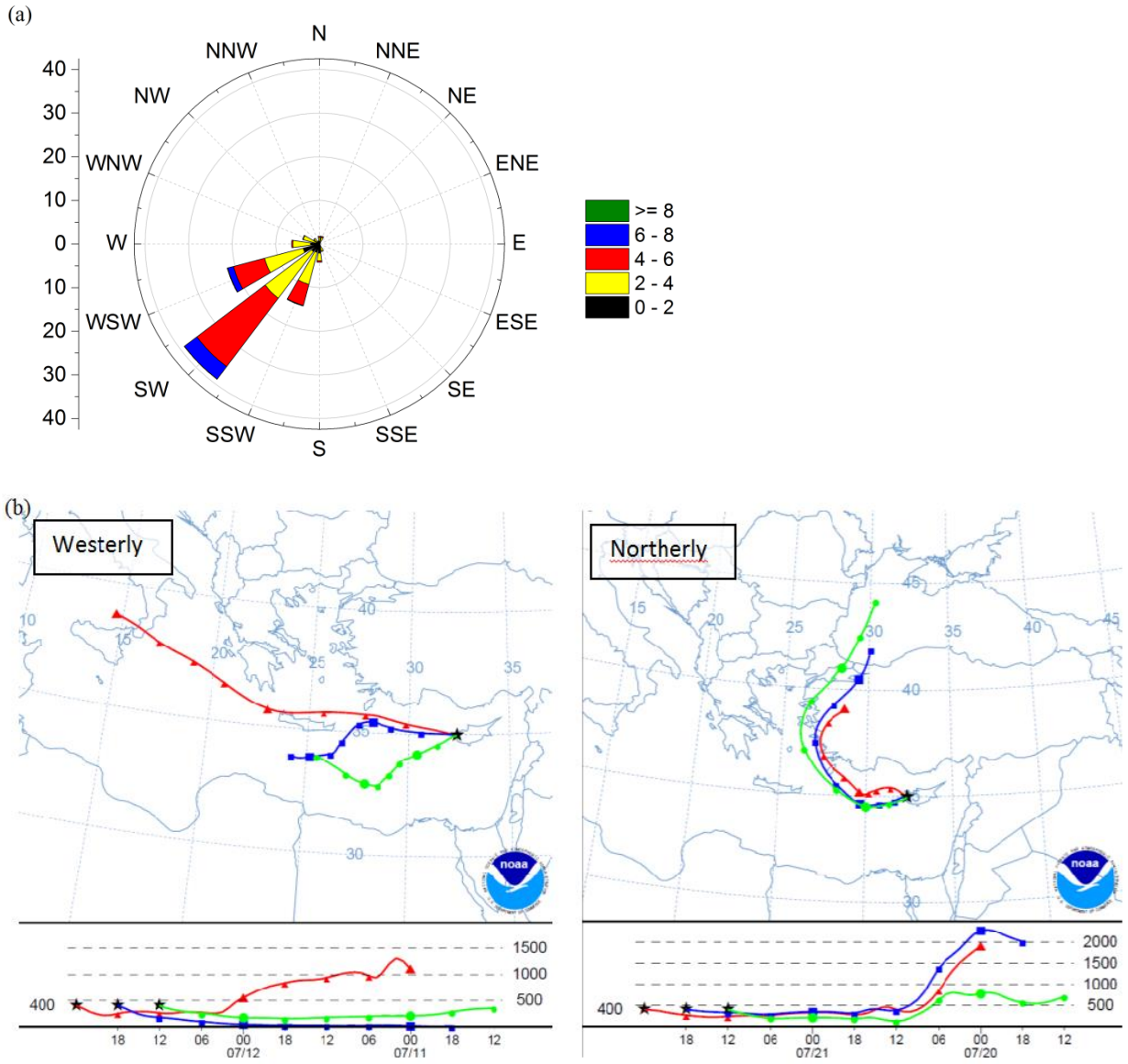

Figure 2: Airflow conditions during the CYPHEX campaign: a) Measured local wind direction, b) back trajectories calculated with NOAA Hysplit model showing examples for the two main air mass origins (48 hours, UTC = LT - 3 h).

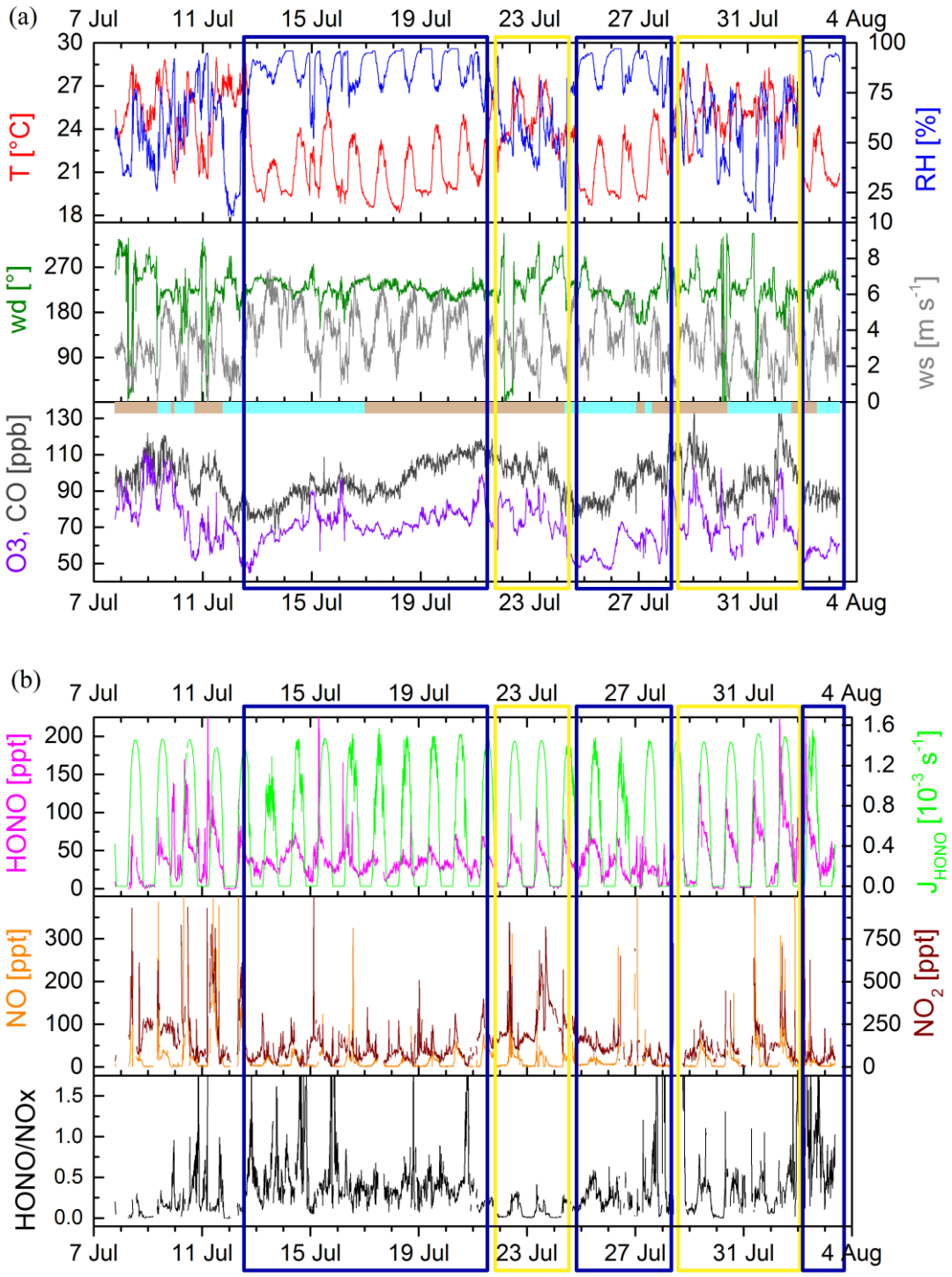

Figure 3: Measured variables during the whole campaign from 7th July to 4th August 2014, a) meteorological data (Temperature T, relative humidity RH, wind direction and speed wd, ws) and O_3 and CO indicating stable conditions, in the lower panel the bar indicates the air mass origin: bright blue = westerly, brownish = northerly, b) observed mixing ratios of HONO, NO_2 and NO, and the photolysis frequency J_{HONO} and the HONO/NOx ratio. The yellow and blue boxes reflect the dry and the humid periods, respectively.

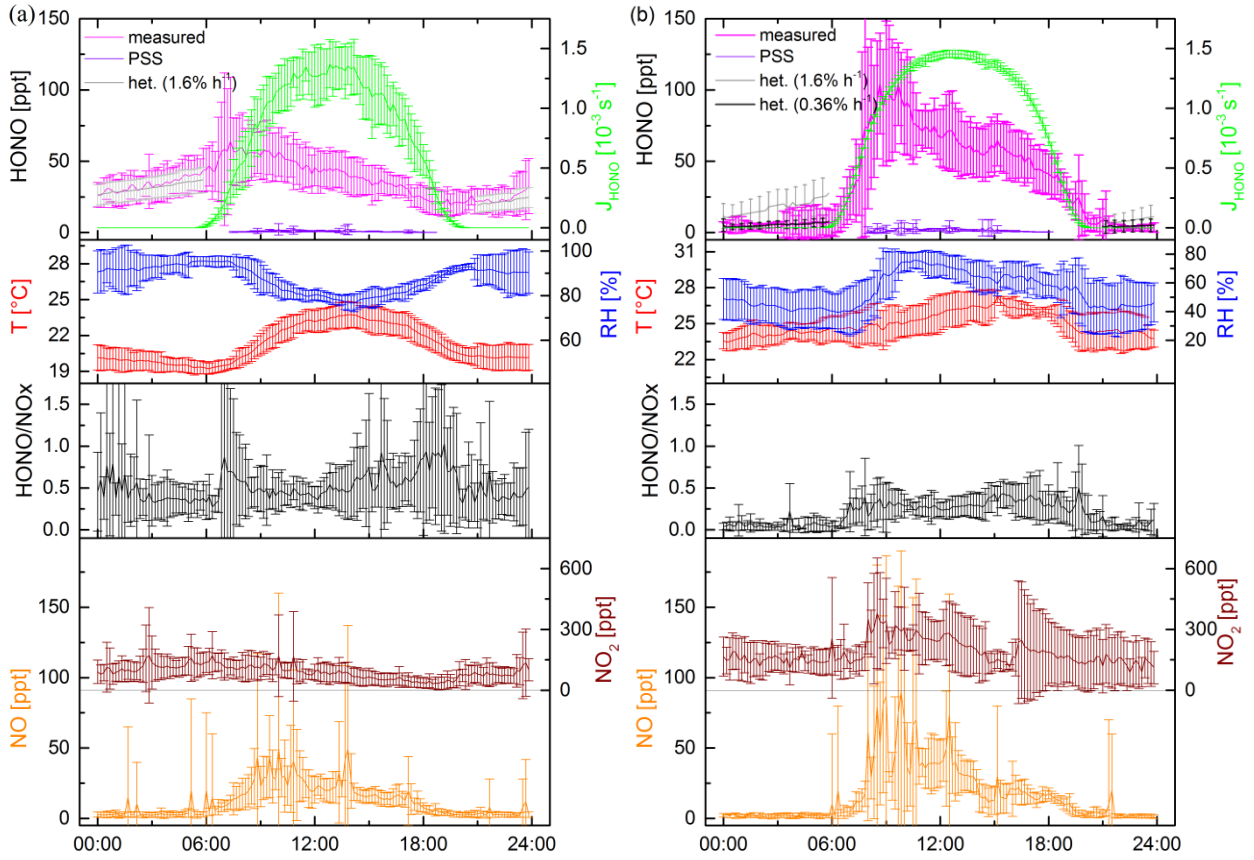

Figure 4: Diel variation of meteorological data (Temperature T, relative humidity RH), NO and NO_2 mixing ratios, the photolysis rate for HONO J_{HONO} and HONO mixing ratios (pink: measured, violet: daytime photostationary state PSS, grey: nighttime heterogeneous NO_2 conversion) and HONO/NOx ratio for a) average for period when RH was above 60% (blue box in Fig. 3) and b) average for dry period when RH was below 60% (yellow box in Fig. 3). Error bars represent standard deviation of diel mean.

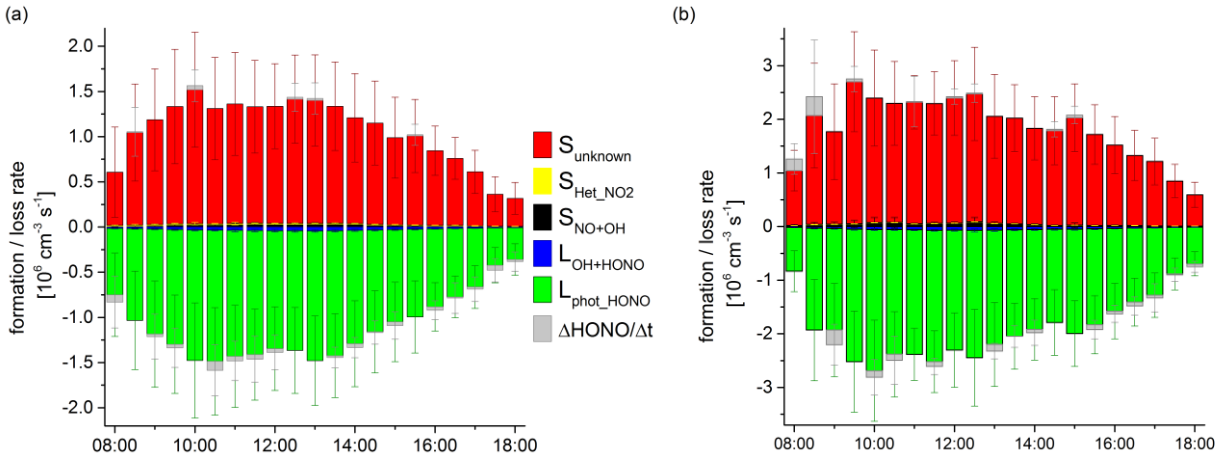

Figure 5: HONO budget analysis for a) the humid and b) the dry period. S_{OH+NO} (black) stands for the formation rate of HONO via the reaction of NO and OH, S_{Het_NO2} (yellow) is the formation rate for the heterogeneous reaction of NO_2 (conversion rate a=1.6% h^{-1}; b=0.36% h^{-1}), L_{phot} (green) and $L_{OH+HONO}$ (blue) are the loss rates via photolysis and the reaction with OH and $S_{unknown}$ is the unknown source. Error bars indicate standard deviation of diel mean.

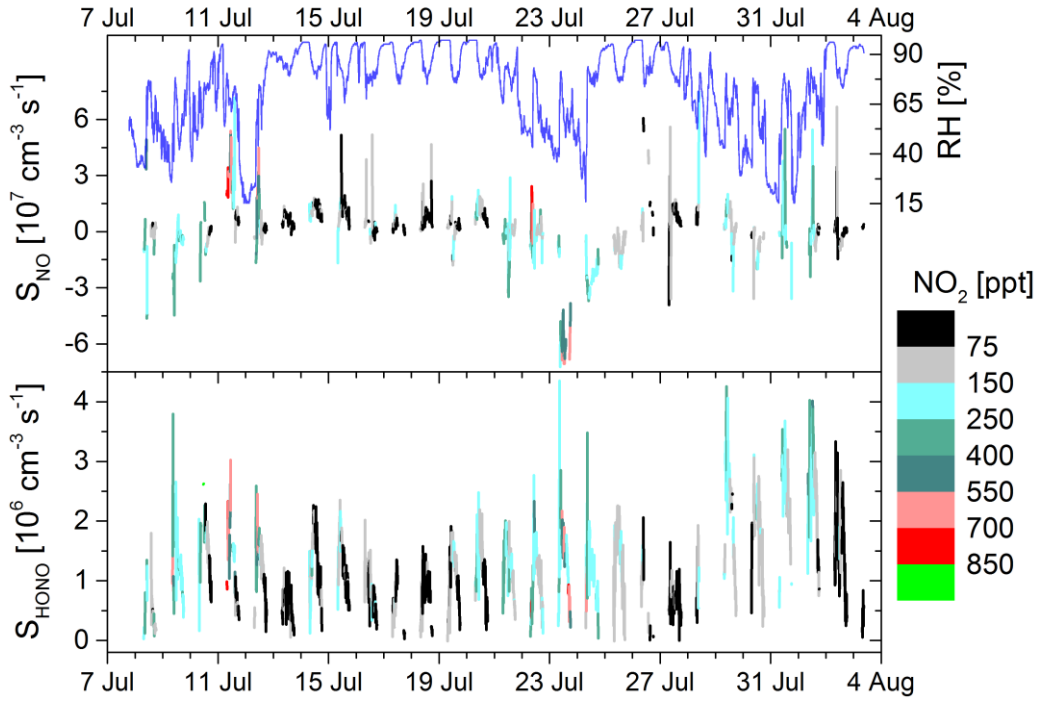

Figure 6: NO_2 (color-coded) and RH dependence of the sources of NO (S_{NO}) and HONO (S_{HONO}).

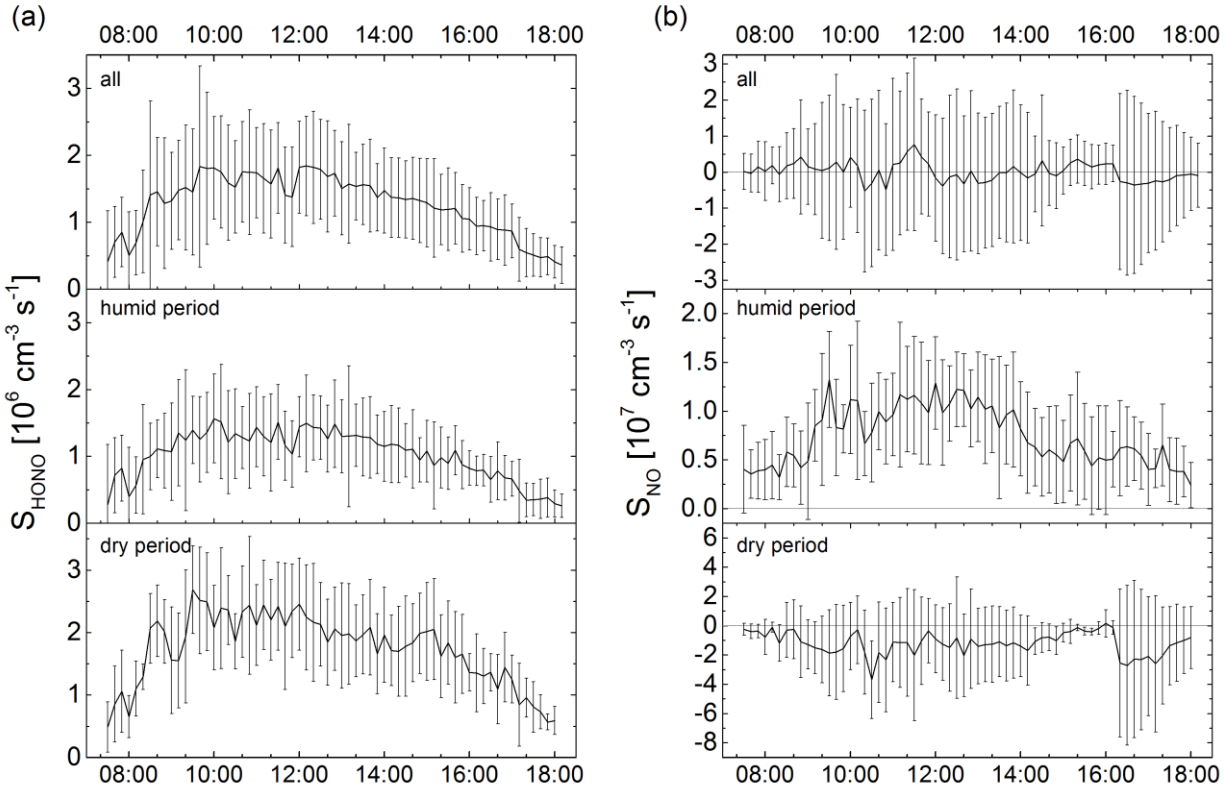

Figure. 7: Diel profile of both unknown sources S_{HONO} (a) and S_{NO} (b) for all data, humid (excluding transition days: 25.7. and 2.8 and 15.7. as RH conditions changed too quickly) and dry periods. Error bars indicate standard deviation of diel average.

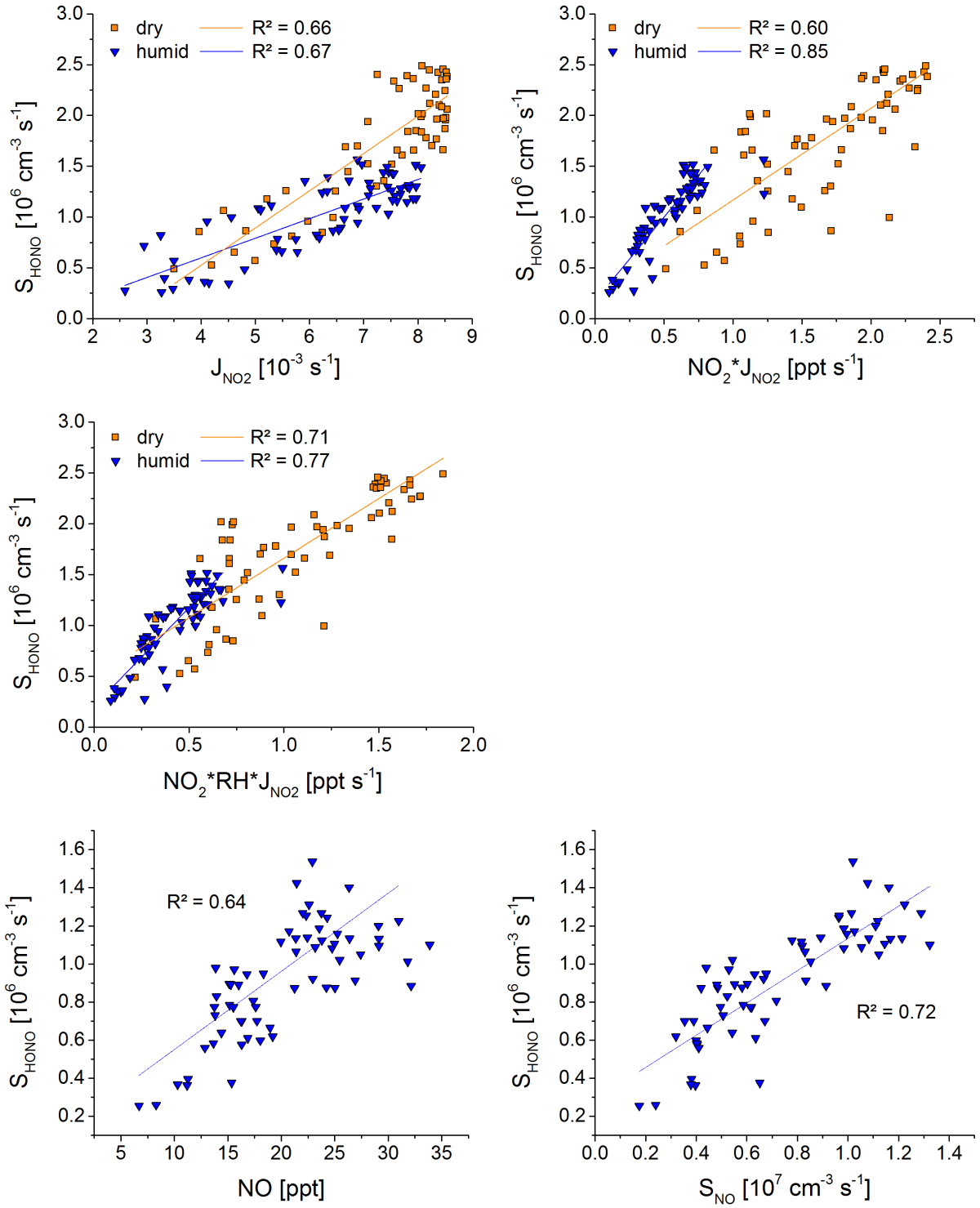

Figure 8: Correlation of S_{HONO} to light induced NO_2 reaction (for both periods, humid = blue triangle, dry = orange square), to NO and S_{NO} (only for humid period, excluding the 3 days mentioned above); time of day average data were used.

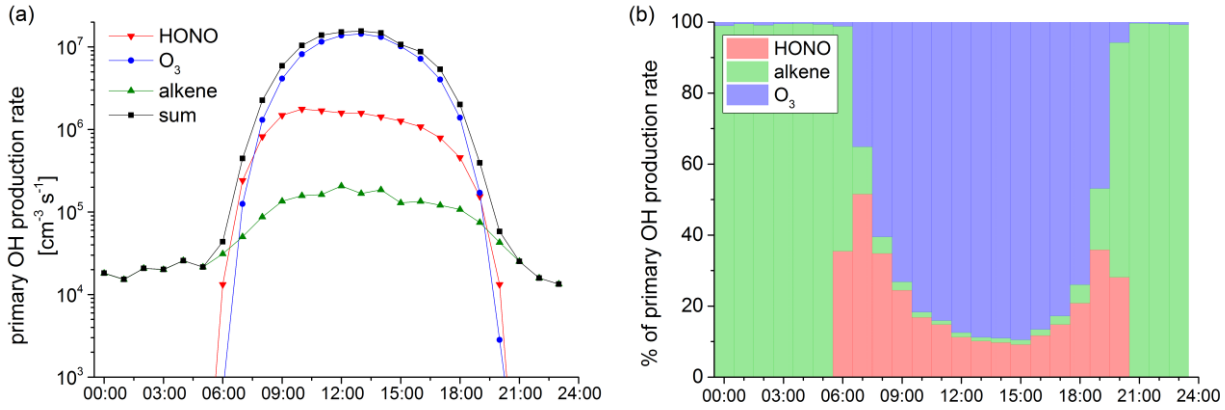

Figure. 9: Average diel pattern of primary OH production from HONO, O_3, and alkenes, shown as a) production rate and b) percentage contributions to primary OH production.